Genomic Islands as minimal hitchers of conjugative elements.

Manuel Ares-Arroyo*, Romane Junker, Amandine Nucci, Marie Touchon, Eduardo P. C. Rocha*
Institut Pasteur, Université de Paris Cité, CNRS UMR3525, Microbial Evolutionary Genomics, Paris, France
*Corresponding authors: manuel.ares-arroyo@pasteur.fr; eduardo.rocha@pasteur.fr.

ABSTRACT

Bacterial chromosomes contain Genomic Islands carrying genes involved in virulence, mutualism, and resistance to antibiotics that are transferred horizontally. Some of them conjugate autonomously (Integrative Conjugative Elements, ICEs), while others use relaxases to hitch on the former's conjugation machinery (Integrative Mobilizable Elements, IMEs). Yet, the mobility mechanism of most Genomic Islands remains elusive. Here, we explore the hypothesis that many carry origins of transfer (*oriT*s) by conjugation. Since very few known *oriT*s were found in ICEs and IMEs, we identified 52 novel families of *oriTs* that cover most integrative elements in 6 major nosocomial species. Most of these *oriT*s are specific to integrative elements, suggesting a clear split in the targets of hitchers of conjugative elements between plasmids and integrative elements. Among 7,363 Genomic Islands, we discovered more than 1,500 IMEs carrying an *oriT* and lacking relaxases and MPF systems. These elements, coined iOriTs, form diverse large ancient families that can be found in different species. These hitchers are genetically unrelated to the putative helpers, beyond the similarity at the *oriT* sequence, and often outnumber them. They include well-known pathogenicity islands, for which the mechanisms of mobility remained unknown. Unlike plasmids, iOriTs have few antibiotic resistance genes, but high density of virulence factors. Like plasmids, the vicinity of *oriTs* concentrates defense and counter-defense systems potentially favoring Genomic Islands dissemination. Hence, iOriTs are frequent integrative mobile genetic elements that evolved to transfer horizontally by hitching on other elements while contributing to bacterial genetic adaptation.

INTRODUCTION

Bacteria are extremely adaptable organisms that have colonized almost every ecosystem on Earth thanks to Horizontal Gene Transfer (HGT), a process in which a bacterium acquires novel traits from other genomes[1]. HGT is usually associated to self-transmissible Mobile Genetic Elements (MGEs), such as a conjugative plasmid or a bacteriophage. Autonomous conjugative elements rely on three components to transfer single-stranded DNA between contiguous cells: the relaxase (MOB), the origin of transfer (*oriT*) and the mating pair formation system (MPF). Conjugation starts when the relaxase recognizes an *oriT*, the only non-coding sequence needed *in cis* to conjugate, where it cleaves one of

34 the DNA strands, binds to it, and carries it to the MPF. The relaxase-ssDNA is transported by the MPF
35 into the recipient cell, where the ssDNA is circularized, and the second strand is synthesized (reviewed
36 in [2,3]). It was observed long ago that most plasmids are not autonomously conjugative[4]. These hitcher
37 plasmids rely on helpers – conjugative elements – to mobilize between cells. Some encode a relaxase
38 and an *oriT* (pMOB) and use the MPF of conjugative elements. Others exploit all the conjugation-
39 related proteins of the latter to conjugate in a process coined *oriT* mimicry[5]. Interestingly, while most
40 of these pOriT have an *oriT* similar to those of conjugative plasmids (pCONJ), and are thus expected
41 to be mobilized by them, many others seem to require a relaxase from a pMOB and a MPF from a
42 conjugative plasmid[6]. Hence, within cells there are complex networks of interdependencies between
43 mobile elements moving by conjugation[7]. Despite receiving less attention than their autonomous
44 counterparts, hitcher MGEs represent a common source of innovation, as they usually encode critical
45 traits for both their bacterial host and helper element[8].

46 Bacterial genomes also carry Integrative Conjugative Elements (ICE). These elements require two
47 additional steps for conjugation: an initial chromosomal excision in the donor cell to establish a
48 transient plasmid-like state from where conjugation starts and a final chromosomal integration step
49 in both donor and recipient cells (reviewed in [9,10]). For these steps, most elements rely on site-specific
50 recombination by Tyrosine recombinases, although ICEs relying on transposable elements and or
51 Serine recombinases have also been characterized[11,12]. The core mechanism of ICE conjugation is very
52 similar to that of conjugative plasmids, and it was shown that most MPF types can be found both in
53 plasmids and integrated in chromosomes[13]. While plasmid conjugation has been the focus of most
54 past studies, the number of ICEs in bacterial genomes often exceeds those of conjugative plasmids[14].
55 Hitchers of conjugative elements can also integrate the chromosome and are called Integrative
56 Mobilizable Elements (IME). Many encode a relaxase and an *oriT* similar to mobilizable plasmids[15],
57 henceforth called iMOB to highlight the analogy to pMOB (Fig 1A), and they were shown to be roughly
58 as abundant as ICEs[14,16]. These elements can only transfer in the presence of conjugative elements[15].
59 Other IMEs encode no protein-coding genes related to conjugation, but carry an *oriT* that is similar to
60 that of helper elements (named iOriT in analogy to pOriT). While plasmids transferring via *oriT* mimicry
61 are abundant in model species[6,17], few examples of iMOB and even fewer of iOriTs have been
62 described (but see [18–20]). As a result, the prevalence and evolutionary significance of iOriTs remains
63 unexplored.

64 Integrative mobile genetic elements provide many adaptive traits to bacteria. ICEs and IMEs spread
65 antibiotic resistance[21], mutualistic traits[22], anti-phage systems[16,23], virulence factors[24], among many
66 other functions. Some ICEs express these functions when dormant in chromosomes, whereas others

67 require previous induction[25], which can be costly[26,27]. Both IMEs and ICEs have commonly been
68 included in the broader term of Genomic Islands (GIs), i.e., chromosomal arrays of accessory genes
69 presumably acquired via HGT and integrated by site-specific recombination[28,29]. GIs have played a
70 pivotal role in the emergence of critical pathogens[30], e.g., *Salmonella* contains multiple Pathogenicity
71 Islands[31] among which some are conjugative[24] or mobilizable[32]. While GIs are extremely abundant[33],
72 and contain may anti-phage defense systems[34], their mechanisms of horizontal transfer are often
73 unknown.

74 In this work, we wished to test the hypothesis that elements mobilizable by conjugation account for a
75 significant fraction of the Genomic Islands in microbial genomes. We focused on six clinically relevant
76 species of Pseudomonodota for which many genomes and MGE-related information is available. Yet,
77 we found very few known *oriT*s in their chromosomes, which led us to identify novel families of *oriT*s
78 by expanding a recently published comparative genomics method for the *ab initio* identification of
79 *oriTs*[35]. We then assessed their presence across Genomic Islands to identify potential functional links
80 between them. Finally, we devised a novel method to delimit them and could thus study the functions
81 of their accessory genes. Our results show that iOriTs are a major class of integrative MGEs, driving
82 the evolution of virulence and MGE-defense, and spreading horizontally thanks to a complex network
83 of interactions with integrative and extrachromosomal elements.

84 RESULTS

85 Conjugative systems and relaxases are abundant in bacterial chromosomes

86 To identify integrative mobile genetic elements potentially transferring by conjugation, we selected
87 six species with a critical relevance in terms of pathogenicity and antimicrobial resistance: *Escherichia*
88 *coli*, *Klebsiella pneumoniae*, *Salmonella enterica*, *Pseudomonas aeruginosa*, *Vibrio cholerae* and
89 *Neisseria gonorrhoeae*. We focused on Pseudomonodota because they have the largest number of
90 available genomes and the best characterized conjugation systems[36]. Across the 6,182 genomes, we
91 identified 16,340 relaxases and 8,391 MPF systems, 10% of which were classed as incomplete.
92 Interestingly, 51% of the relaxases and 42% of the MPF systems were encoded in chromosomes (Fig
93 1B), despite the latter being twice less common than plasmids (6,284 chromosomes, 13,090 plasmids).
94 Many chromosomes (41%) encode more than 1 relaxase or even MPF (8%), which is rare in plasmids
95 (<2%, Fig 1C-D), suggesting they have multiple MGEs mobilizable by conjugation. *V. cholerae* is the
96 only species in the dataset with two chromosomes and all MPFs were identified in the larger
97 chromosome (Fig S1). The frequency of putatively inactivated conjugative systems is higher in
98 chromosomes (15.6%) than in plasmids (5.7%) (Fig 1E). Most plasmids in these species are of MPF

99 types F, T and I, of which only ~5% are incomplete, whereas chromosomes harbor MPF types G and T
100 among which 10% and 26% respectively are classed as incomplete mostly due to the lack of the
101 essential ATPase *virB4* (Fig S2). It is possible that defective elements integrated in chromosomes are
102 more stably maintained in genomes than defective plasmids, which may be easily lost by segregation.

103 Our first analysis revealed that we were lacking the relaxase of the *Salmonella* Genomic Island 1[37].
104 When enquiring on the reasons of these results, we realized that the widely used programs to identify
105 relaxases systematically miss one type of relaxase: MOB_M. We made a novel protein profile, now
106 added to CONJscan (see Methods), and this revealed an unprecedented abundance of ICE/IMEs with
107 relaxases from the MOB_M family (not to be mistaken with the *mobM* gene in *Staphylococcus aureus*
108 from the MOB_V family[38]). MOB_M relaxases were found to be the most common in the chromosomes,
109 even if we could only find three previous descriptions in the literature (pCW3, SGI1 and pIGRK)[37,39,40].
110 MOB_M relaxases are distantly related to tyrosine recombinases, the existing protein profiles missed
111 them systematically, and they were almost exclusively found in chromosomes (Fig 1G). This may
112 explain why they were previously overlooked and occasionally annotated as integrases. The use of an
113 accurate protein profile revealed that 96% of the MOB_M relaxases are located nearby an integrase (see
114 below). They are specifically associated to MPF type G (44%, ICEs) or in iMOBs (56%). Hence, even in
115 well-studied clades some relaxases are missed, which may result in an under-estimate of iMOB
116 elements.

117 To associate the genes encoding relaxases and MPFs to integrative elements, we first identified the
118 Genomic Islands across the genomes using the consecutive persistent gene families as delimitation.
119 This limits MGEs to specific intervals, which can be grouped across a species in spots (see Methods),
120 to identify similar locations across genomes[41]. Genomic Islands encoding MPF and/or relaxases
121 defined by the edges of the intervals are henceforth called interval-delimited Genomic Islands (GI^{id})
122 (Fig 1F, Fig S3A). In our dataset, 90.5% of the relaxases and 90.7% of MPF systems are located within
123 GI^{id}s. The remaining ones are in intervals where large rearrangements took place and cannot be
124 assigned non-ambiguously to spots. An interval may have multiple GIs, but this should be rare since
125 most GI^{id}s encode only one relaxase (92.7%) and one MPF (>99%). In 81% of the cases, the interval
126 with an ICE/IME had at least one integrase (68% only one) (Fig S3). Most intervals lacking an intact
127 integrase had an integrase pseudogene (81%). This suggests that the coincidence between the MGE
128 and the interval is high. Using this delimitation, we can separate within the chromosome the relaxases
129 in those associated with a MPF that is complete (ICE, 53%) or incomplete (dICE, 6%), from those that
130 are alone (iMOB, 41%). Previous works had found roughly similar numbers of ICE and IME across
131 bacteria[14,16] matching what is observed in plasmids[42]. Yet, in our focal species we found 1.47 times

132 more iMOBs than ICEs (Fig 1H). The very large number of MOB_M relaxases may explain why we found
133 a much larger number of relaxases than previous works. These results show that hitchers encoding
134 relaxases are more frequent among integrative conjugative MGEs than among plasmids.

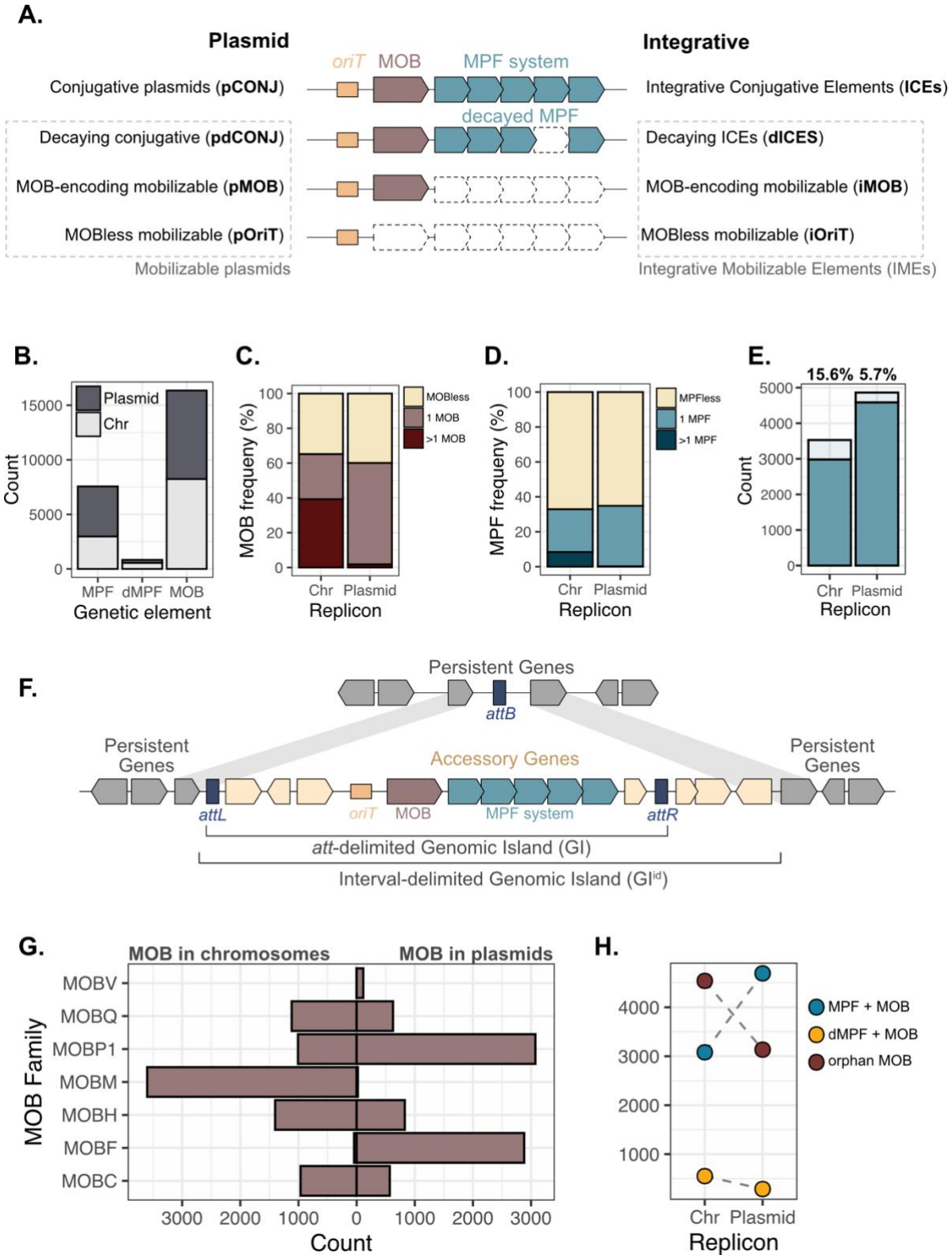

135
136

Figure 1. A. Definition of MGEs. In the middle, the genetic elements responsible for conjugation. *oriT*: origin of transfer, MOB: relaxase; MPF: mating pair formation system. At the left, MGE definition when the genetic elements are found in episomal replicons. At the right, when integrated into the chromosome. **B.** Number of genetic elements identified. dMPF: decaying MPF. **C.** Frequency of replicons carrying none, one, or more than one relaxase. Chr: chromosome. **D.** Frequency of replicons carrying none, one, or more than one MPF system. **E.** Number of complete MPF systems (dark blue) and incomplete (light blue). The number indicates the percentage of incomplete MPF systems in chromosomes and plasmids, respectively. **F.** Schematic representation of an interval-delimited and *att*-delimited Genomic Island within a spot. **G.** MOB families identified in plasmids (right) and chromosomes (left). **H.** Count of relaxases found in chromosomes (left) and plasmids (right) associated with a MPF, decaying MPF or none MPF. Grey dashed lines connect the same element in the different replicons.

Origins of transfer in chromosomes are different from the *oriTs* known in plasmids

Plasmids encoding no relaxases or MPF while carrying *oriTs* (i.e., pOriTs, Fig 1A) represent a large fraction of plasmids[6]. In contrast, only few IMEs lacking relaxases (iOriTs) are known to carry an *oriT*[18–20]. We searched for known families of *oriTs* and found 9,647 instances in the genomes, 83% of them in the plasmids (Fig S4). Since relaxases are expected to have a cognate *oriT* in the element and there are more relaxases in chromosomes than in plasmids, these results show that we are missing most of the *oriTs* used by the integrative elements. Indeed, while we could identify an *oriT* in most of the relaxase-carrying plasmids (~70% of pCONJ, pdCONJ, pMOB), we found very few in relaxase-carrying GI^{id}s: 30% in ICEs, 15% in dICEs and almost none in iMOBs (Fig 2A). Since we missed *oriTs* even in cases where one should expect to find them (ICEs and iMOBs), this means that integrative elements and plasmids use different *oriT*s and that most of the former are unknown.

We applied our recent method to identify novel families of *oriTs* when there is no prior knowledge on their sequences[35]. Briefly, we retrieved the first large intergenic sequence upstream of every relaxase, which is the most usual location of *oriTs*, and clustered them based on their nucleotide identity while accounting for the type of relaxase (see Methods). We identified 76 candidate *oriT* families, of which a third included *oriT* sequences previously described in the literature. The remaining 52 are completely novel *oriT* families (Fig 2B), and were named according to their associated MOB family with a numeric identifier. To distinguish them from delimitated *oriT* sequences, an additional '*r*' standing for '*region*' was added to the name (e.g., $oriT_{rQ1}$, $oriT_{rQ2}$) (see Methods). Six previously identified *oriTs* in our first screening could not be identified by our method, presumably because they are too rare to form an *oriT* family (0.06% of the *oriTs* in our previous analysis, Fig S4). Five *oriT* families are known to be absent of the intergenic region upstream the relaxase in these species, but far from any relaxase gene, e.g. $oriT_F$ which is next to a relaxosome-accessory protein at the opposite edge of the conjugation operon in F plasmids[43]. These *oriTs* were added manually (see Methods, Fig 2B). Finally, we built HMM DNA profiles for every known and new *oriT* candidate and used them to find occurrences in the 6,182 genomes. We identified 21,516 putative *oriTs* in both plasmids (56%) and chromosomes (44%).

175 We identified 4,217 *oriTs* using HMM profiles of known families, 40% of which were missed by pairwise
176 sequence alignments (Fig 2D-E), highlighting the higher sensitivity of the HMM approach. The majority
177 of the chromosomal *oriTs* were of the novel types (62%) (Fig 2C). The fraction of relaxase-encoding
178 integrative elements with a candidate *oriT* increased to 93.5%, suggesting that we uncovered most
179 *oriT*s in these species (Fig 2A). As expected, >99% of the MGEs carry the *oriT* next to the relaxase (<5Kb
180 distance), once we accounted for the known exceptions (e.g., $oriT_{ICEclc2}$, $oriT_{F}$). Most plasmids (83%)
181 and GI^{id}s (85%) with an *oriT* carried just one (Fig S5), with the others often having two copies of the
182 same family, suggesting they are in plasmid dimers or co-integrates. The similarity of trends between
183 plasmids and GI^{id}s suggests the multiplicity of *oriT*s is not caused by mis-delimitation of the latter (Fig
184 S5A-B). Some of these cases were previously described in individual plasmids (e.g., two $oriT_{R6K}$)[44] and
185 ICEs (e.g. $oriT_{ICEclc1}$ & $oriT_{ICEclc2}$)[45]. To assess if the novel *oriT*s cover most conjugative elements in a
186 dataset independent from the one used to characterize them, we retrieved the 2,289 genomes of the
187 six species submitted from June 2023 to May 2025. In this novel dataset, we identified 2,942 relaxases
188 in the chromosomes and 92% of them were next to one of the *oriTs* identified (Fig S6). This suggests
189 we covered most of the *oriT* diversity of these species.

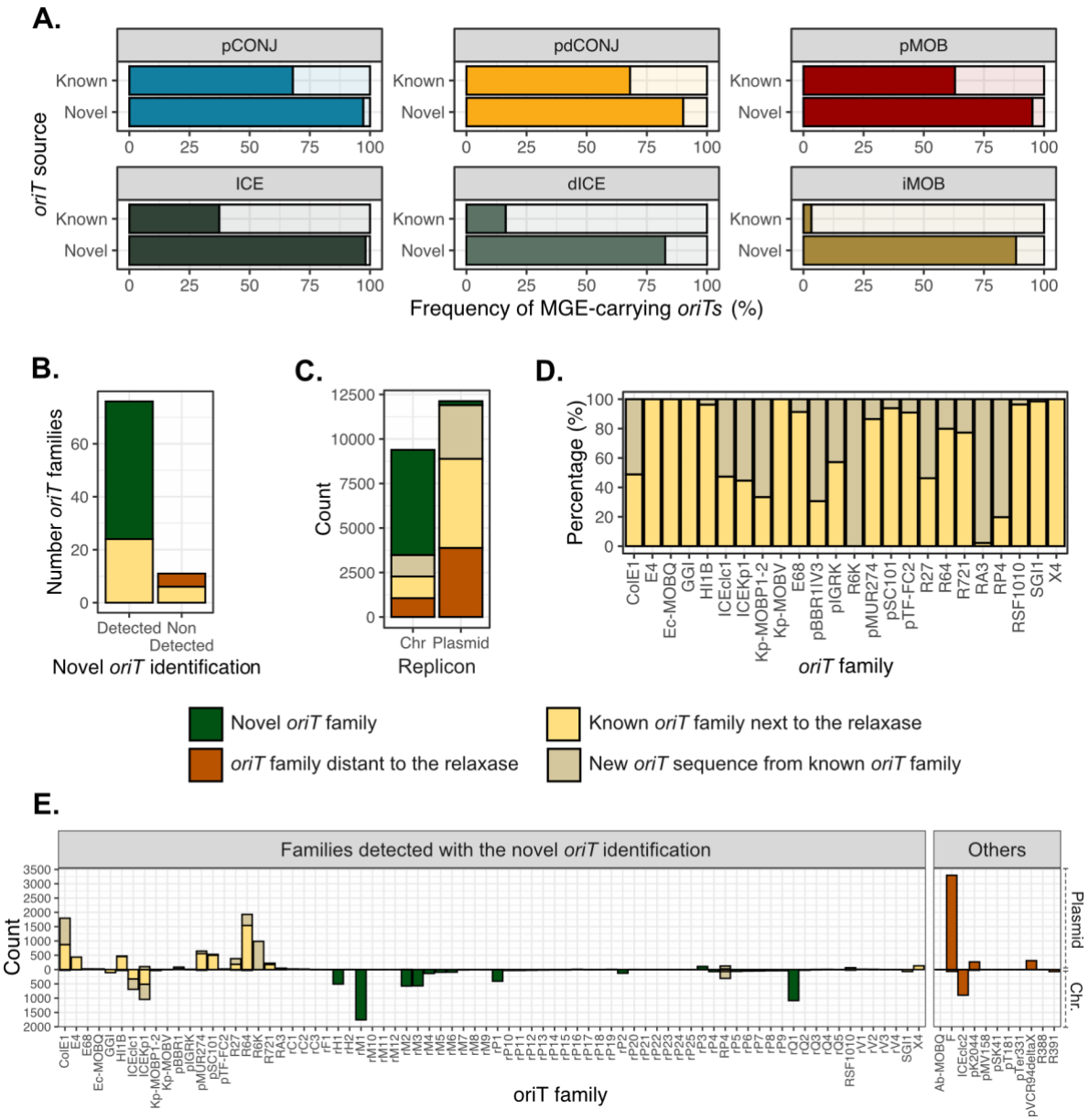

Figure 2. A. Frequency of relaxase-encoding elements with an *oriT*. Known, stands for *oriTs* already known in the literature. Novel, *oriTs* identified in this work. **B.** Number of *oriT* families detected and non-detected by our method. The color indicates the source of the *oriT*. **C.** *oriT* occurrences across chromosomes and plasmids. **D.** Known *oriT* families that were also detected by our method. The percentage indicates the fraction of new occurrences. **E.** The number of *oriT* families found in plasmids and chromosomes, the legend indicating the source of the *oriT*.

Integrative elements carrying only *oriTs* are frequent in bacteria

Elements carrying only an *oriT* must interact with a relaxase encoded in the helper to be transferred by conjugation[5]. Since we can now identify most MOB-associated *oriT*s, we can also identify the integrative hitchers carrying only *oriTs* (iOriT): they should have an *oriT* similar to the one of the helper carrying the relaxase. We examined the 9,930 *oriTs* located in chromosomes and found 94% within the GI^{id}s (Fig S7), as expected since ~90% of relaxases and MPF systems are in these locations (see

204 above). Around 76% were identified in GI^{id}s containing relaxases (i.e., ICEs, dICEs, iMOBs) and 1,750
205 *oriTs* were found in GI^{id}s lacking relaxases or MPF systems, i.e. in iOriT (Fig 3A). Altogether, we
206 identified 7,363 GI^{id}s corresponding to integrative elements, both ICEs, dICEs, iMOBs and iOriTs (Fig
207 3A). The latter often co-occur in the genomes (up to nine integrative elements in the same *P.*
208 *aeruginosa* chromosome (NZ_LS998783.1)). iOriTs represent a large fraction of the IMEs (37%) and of
209 all integrative MGEs associated with conjugation (24%). The integrative hitchers (IMEs: iOriT and
210 iMOB) are almost double the number of autonomous elements (ICEs, Fig 3A). To note, the IME/ICE
211 ratio varies extensively across the taxa, with IMEs outnumbering ICEs in some species (*E. coli*, *S.*
212 *enterica*), while being rarer in others (*P. aeruginosa*, *N. gonorrhoeae*, Fig 3B). Mobilizable plasmids
213 (pOriT, pMOB) are more numerous than IMEs (iOriT, iMOB) in our dataset (Fig S8). Yet, this is only true
214 for half of the species (*Ec*, *Kp* and *Ng*), the opposite being observed in the others (*Se*, *Vc* and *Pa*), where
215 iOriTs alone are more abundant than the whole sum of mobilizable plasmids (Fig 3B, Fig S8). In
216 conclusion, iOriT are numerous and together with iMOB they often make the largest fraction of
217 integrative elements transferable by conjugation, even if their abundance seems to vary between
218 species.

219 The log-transformed size of plasmids follows a very characteristic bimodal distribution, where
220 conjugative elements are large and mobilizable elements are bimodal[6]. While it has been observed
221 that the median size of conjugative plasmids is slightly higher than ICEs[46], little is known about the
222 distribution of size of integrative hitchers. To obtain a more precise delimitation of the elements, we
223 searched for the elements' *att* sites (Fig 1F). We found them for 58% of the integrative elements (4,298
224 out of 7,363 elements, see Methods) (Fig S9). Almost all of these *att* sites (99%) matched those
225 recently provided in the TIGER *att* database[47], which uses a different method to identify them,
226 supporting the validity of our predictions (Fig S9, Table S1). In the same genomes analyzed by both
227 our work and the TIGER database, 86% of our *att*-delimited GI match those found by TIGER even if the
228 latter are not focusing on hitchers by conjugation (they found 95% of the ICEs in this work, but 95% of
229 iMOBs and 98.3% iOriTs were just classed as 'other GI'). As expected, an integrase was encoded in the
230 2Kb vicinity of 92% of the *att*-delimited GIs (hereinafter GIs), which in most cases encoded one and
231 only one intact recombinase gene (82%) (Fig S9). Only 6% GIs lacked detectable vestiges of these
232 genes. Integrases of the Serine recombinase family were very rare (<1%). GIs delimited by *att* sites are
233 necessarily equal or smaller than those delimited by the intervals. In 80% cases, the GI retained more
234 than 80% of the length of the original GI^{id} (Fig 3C). In cases where the GI was much smaller than the
235 one delimited by intervals (low GI/GI^{id} ratio), additional MGEs were found integrated in tandem in the
236 spot (Fig 3D). This indicates that intervals provide a reasonable approximation of the integrative MGEs,
237 but that *att* site identification is important for their accurate delimitation.

238 The GIs show characteristic size distributions (Fig 3E). In agreement with previous works[48], ICEs are
239 large (mean of 75Kb) and their size varies with their MPF type: from the 100Kb MPF_F ICEs to the 56Kb
240 MPF_T (Fig S10). Decaying ICEs are on average smaller (65Kb) than ICEs and the distribution of their
241 sizes reveals a longer left tail suggesting that many were partially deleted (Fig 3E), as observed in
242 plasmids with incomplete conjugative systems[49]. The iMOBs are small (23Kb) whereas the iOriTs show
243 a bimodal distribution with many elements being more than 50kb long (Fig 3E). Inspection of the large
244 iOriT revealed well known and precisely delimited genomic islands (Fig S11). The difference in size
245 distribution between iOriT and iMOB is surprising, since both pMOB and pOriTs show bimodal
246 distributions with both large and small elements[6]. While the size distribution of iOriT is the expected
247 one, large iMOBs are rare in these species.

248 The present data allows to compare for the first time the size of integrative and plasmid elements
249 transferrable by conjugation. Integrative elements show a narrower size distribution (interquartile
250 range 22-79Kb) than plasmids (6.1Kb-116Kb), with iMOBs being on average larger than pMOBs
251 (Kolmogorov–Smirnov test: $D = 0.54$, $p < 2.2^{-16}$) and ICEs shorter than pCONJ ($D = 0.35$, $p < 2.2^{-16}$).
252 These differences are due to two effects. Among the small elements, some plasmids are extremely
253 small (down to <1kb), whereas integrative elements are always larger than 4kb (one single 2Kb
254 exception). This may be because the integration module requires the presence of integrases,
255 excisionases and *att* sites, whereas plasmids only require an origin of replication and can therefore be
256 much smaller. Among conjugative elements, the differences seem to be found at the right end tail of
257 the distribution since some plasmids are extremely large (up to >1Mb), which is never the case of ICEs
258 in our dataset.

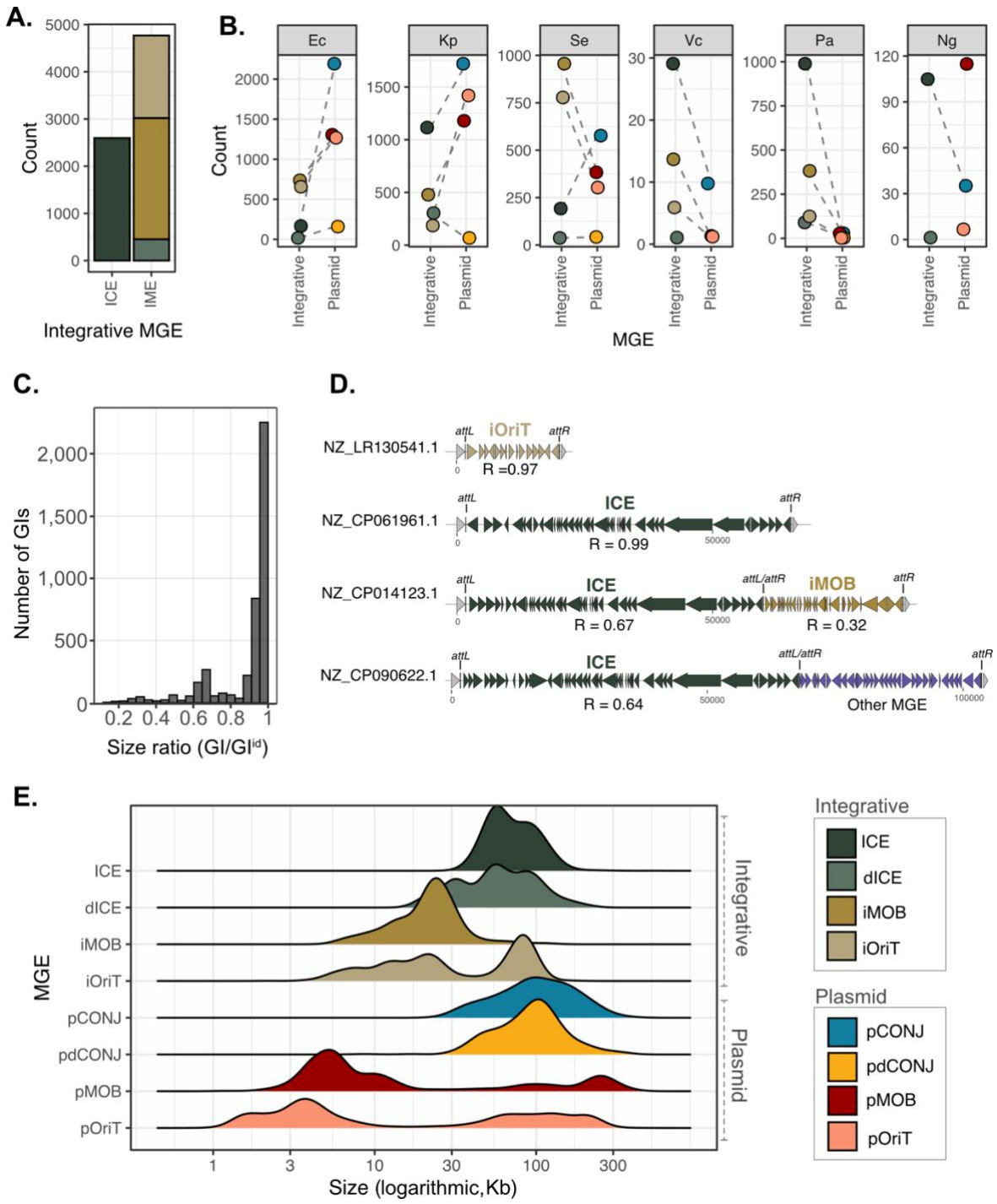

Figure 3. A. Number of integrative MGEs, both autonomous ICEs and hitcher IMEs (dIMEs + iMOBs + iOriTs). **B.** Number of integrative elements (ICE, dICE, iMOB, iOriT) compared to the number of plasmids (pCONJ, pdCONJ, pMOB, pOriT) in the six species. Dashed grey lines link MGEs carrying the same conjugative elements (ICE-pCONJ; dICE-pdCONJ; iMOB-pMOB; iOriT-pOriT). Ec: *E. coli*; Kp: *K. pneumoniae*; Se: *S. 11lasmid11*; Vc: *V. cholerae*; Pa: *P. aeruginosa*; Ng: *N. gonorrhoeae*. **C.** Size ratio of *att*-delimited Genomic Islands against interval-delimited Genomic Islands. **D.** Examples of the same genomic spot occupied by different MGEs alone or in tandem. The MGE type is annotated over the element, whereas the size ratio (GI/ GI^{id}) appears under it. **D.** Size distribution of MGEs. The size is represented after a logarithmic transformation.

269 ## iOriTs depend on co-occurring ICEs and conjugative plasmids to transfer

270 The functional dependencies of IMEs, i.e., which helper MGEs they exploit, are mostly unknown. Some
271 IMEs are known to transfer by hijacking the conjugative machinery of ICEs (e.g., the iOriT
272 MGI*Vfl*Ind1)[50], whereas others hijack conjugative plasmids (e.g., the iMOB SGI1)[51]. Inversely, some
273 ICEs mobilize plasmids[52–54]. One can identify putative iOriT helpers by searching for *oriT* sequence
274 similarity. In plasmids, *oriT* families are usually either in pCONJ (and pdCONJ) or pMOB, but not in both
275 (Fig 4A). We found that the same applies to integrative MGEs: *oriT* families are usually associated to
276 either ICEs (and dICEs) or iMOBs, but none is found in both (Fig 4A). Accordingly, the iOriTs usually
277 have *oriT*s of the same families as those found in either ICEs or iMOBs, but not both (Fig 4B). Hence,
278 while some plasmid and integrative hitchers carrying just an *oriT* for conjugation exploit both the
279 relaxase and MPF of a conjugative element (two thirds of the cases) (Fig 4C-D), a third of them exploit
280 a relaxase from another hitcher (iMOB/pMOB) and a MPF from a conjugative element (Fig 4C-D). The
281 latter require the presence of two different compatible MGEs in the cell.

282 The observation that plasmid *oriT*s are rarely found in chromosomes (Fig 2E, Fig S4), suggests a split
283 of *oriT* families between integrative elements and plasmids. Indeed, the vast majority of *oriT* families
284 of elements encoding a relaxase are specialized: either they are found in plasmids or in integrative
285 elements (Fig 4A and 4D). The frequency of iOriT and pOriT in each *oriT* family confirms the rule that
286 *oriT* families tend to be specialized in terms of the type of MGE (integrative or plasmid), most
287 exceptions caused by very low counts for these *oriTs* in MOBless elements (Fig 4E). Only few *oriT*
288 families are found at appreciable frequency in both types of elements (coined "*shared oriTs*" in Fig 4A-
289 C) and only two are frequent (Fig 4F): $oriT_{RP4}$ which is found in many pCONJ and iMOB, and $oriT_{ICEKp1}$
290 which is found in many ICEs and pCONJ (Fig 4A). Interestingly, they are also found in many MOBless
291 elements, but almost exclusively in iOriT (nearly absent in pOriT), suggesting complex interactions
292 between some GIs and plasmids.

293 To detail the interdependencies between different MGE types, we retrieved all *oriT* families with >10
294 occurrences in our dataset and built a graph with the number of *oriT* families than can be found in two
295 different types of MGEs. Our results show that plasmids are highly interconnected, *i.e.,* pOriTs heavily
296 rely on other plasmids for their mobility (Fig 4D, Fig S12). In contrast, iOriTs have *oriT*s from families
297 present in ICEs and pCONJ (Fig 4D). Among the iOriTs, 335 have an ICE-like *oriT*, 205 have an iMOB-
298 like *oriT*, 265 have *oriT*s of families with multiple origins ("*shared oriTs*"), and only 30 have a plasmid-
299 like *oriT*. This result suggests that ICEs and IMEs drive the transfer of most Genomic Islands lacking
300 relaxases, but some conjugative plasmids may also contribute to their mobility. In contrast,

interactions between iOriT and pMOB or between pOriT and iMOB can occur (Fig 4D), but are rare (Fig 4C).

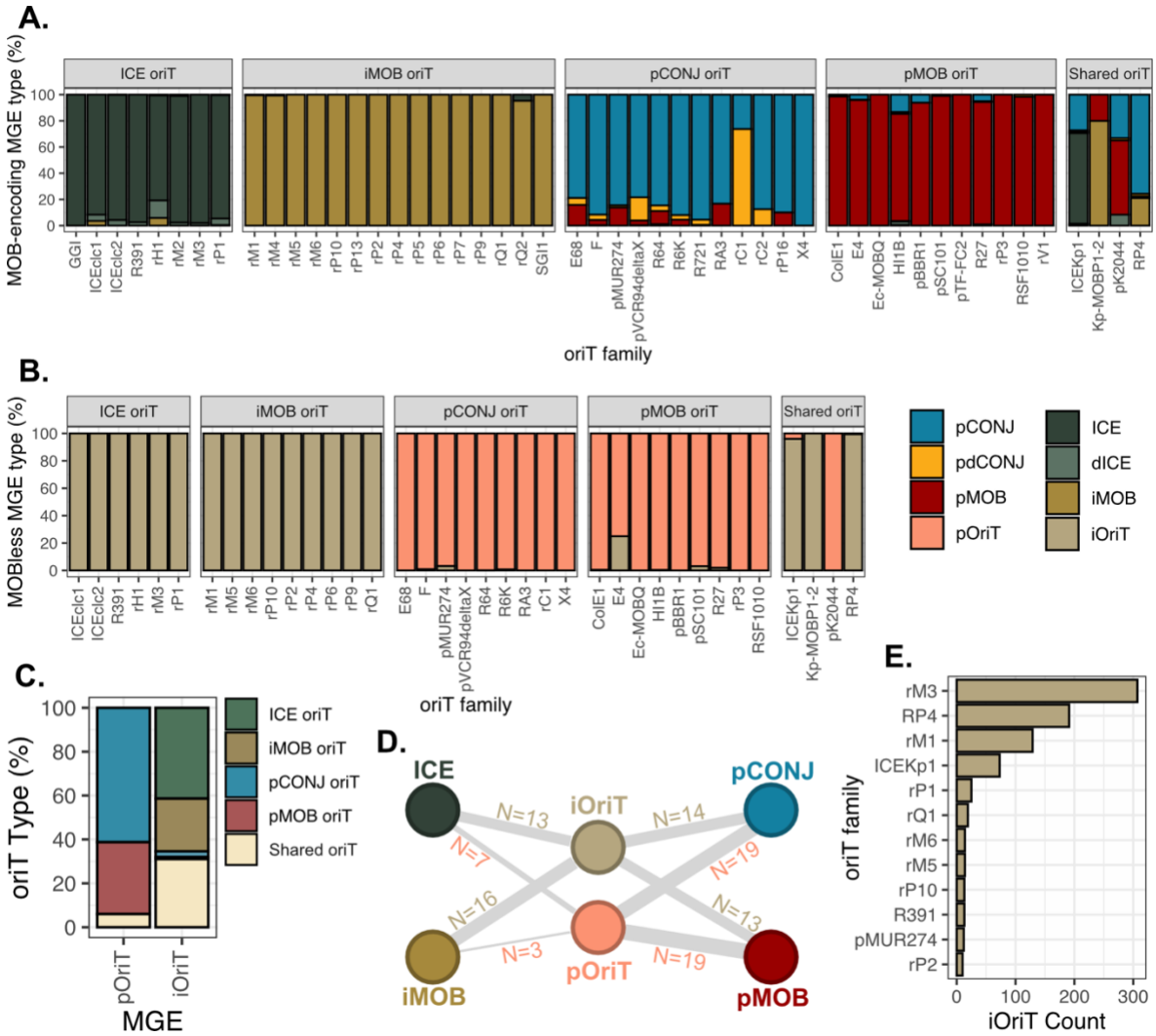

Figure 4. A. Frequency of MGE types carrying a relaxase in which an *oriT* family has been identified. The *oriTs* were split into 'ICE *oriT*', 'iMOB *oriT*', 'pCONJ *oriT*' and 'pMOB *oriT*', according to the most common MGE associated to the family. A fifth group 'Shared *oriT*' contained those associated to different MGEs. Only *oriT* families with 10 or more occurrences in the dataset are shown. **B.** Frequency of MOBless MGEs in which an *oriT* has been identified. Only *oriT* families with 10 or more occurrences in the dataset are shown. The *oriTs* were grouped into the same five categories as 4A. **C.** Percentage of *oriT* categories carried by pOriTs and iOriTs. **D.** Graph showing the number of *oriT* families with >10 occurrences shared between MOBless elements and pCONJ, pMOB, ICE and iMOB. The nodes of the graph represent the MGEs. Edges connect MGE types when a same *oriT* has been found in both elements, its width representing the number of different *oriTs* in common. The number is shown next to the edge. **E.** Number of *oriT* families associated to iOriTs. Only cases with >10 iOriTs are shown.

iOriTs form large families of MGEs

The above data suggests that iOriTs are specific families of MGEs with importance in bacterial evolution. Alternatively, iOriTs might just be decaying MGEs that recently lost conjugation-associated protein coding genes. If so, then iOriTs should be intermingled in families of ICEs and IMEs. To test this

321 hypothesis, we computed the weighed Genetic Repertoire Relatedness (wGRR, see Methods)
322 between the 4,298 *att*-delimited ICEs and IMEs and the 10,492 conjugative and mobilizable plasmids
323 (discarding 773 phage-plasmids and 1,825 non-transmissible ones) (Fig S13). Briefly, wGRR=1 means
324 two elements have identical genetic repertoires, or one element is a subset of the other, as expected
325 if one is decaying, whereas wGRR=0 indicates lack of homologous genes. We found 590 elements with
326 no wGRR hit with other element in the dataset. The remaining 14,200 elements were clustered into
327 438 communities using the Louvain algorithm on the wGRR matrix (see Methods). Since most
328 communities had few elements, we retrieved the 181 communities with more than 5 elements for
329 further analysis (including 13,442 elements) (Fig S13). In most of these communities, more than 75%
330 of the elements are of the same MGE type (N=161/181). The 723 iOriTs were found in 41 communities,
331 of which 21 iOriTs were in those dominated by other MGEs (mostly iMOBs). A set of 87 iOriTs
332 accounted for ~50% of the elements of eight mixed communities, in which case the whole community
333 typically shared the same *oriTs* family. These cases of iOriTs highly similar to iMOBs could be due to
334 recent events of MOB loss in the former. In contrast, 615 iOriTs constituted 19 communities where
335 they were the only or the most numerous element (Fig 5A, Fig S14). Among these communities, four
336 had elements from two or three different species (Fig S15), showing inter-species dissemination of
337 highly related iOriTs. These results suggest that while some iOriT may have recently derived from
338 iMOBs, most iOriTs are in large families of similar types of elements.

339 To explore the functional dependencies of iOriTs, we built a graph in which each node represents a
340 community and edges connect communities with the same origin of transfer (Fig 5A). This revealed
341 pairs of families of putative hitcher and helpers that have similar *oriTs* but very different genetic
342 repertoires (e.g., see clusters with *oriTs* rM3, RP4, ICEKp1) (Fig 5A). For instance, iOriTs with the $oriT_{rM6}$,
343 are the TAI islands identified in *E. coli* O157:H7 in 2002, whose transfer mechanism remained unknown
344 until now[55]. Remarkably, their *oriT* region is 60% identical to the one recently reported in the ICE SGI-
345 4[56], whose MOB_M relaxase had not been identified prior to this study. These iOriTs have almost no
346 sequence similarity to the ICEs able to mobilize them beyond the *oriT* region (Fig 5B). In other cases,
347 the hitcher-helper pairs are very different in size and may even differ in terms of vertical transmission
348 (some are integrative, and the others are plasmids). For instance, different families of small iOriTs and
349 iMOBs carry the same *oriT* family as the well-known conjugative plasmid RP4 (Fig 5C), and have been
350 simultaneously found across other Pseudomonodota[57]. This is often the only region of similarity
351 between the different types of elements. Lastly, there are iOriTs with *oriT* families found in both ICEs
352 and pCONJ, which suggests they may exploit one or both types of elements. This is the case of small
353 iOriTs carrying the $oriT_{ICEKp1}$ also found in the ICE*Kp1* described in *K. pneumoniae* in 2008[58] (Fig 5D),

354 and also carried by conjugative plasmids (Plasmid Taxonomic Unit PTU-E50) (Fig 5C). None of the three
355 groups of elements shows high sequence similarity beyond the *oriT*s.

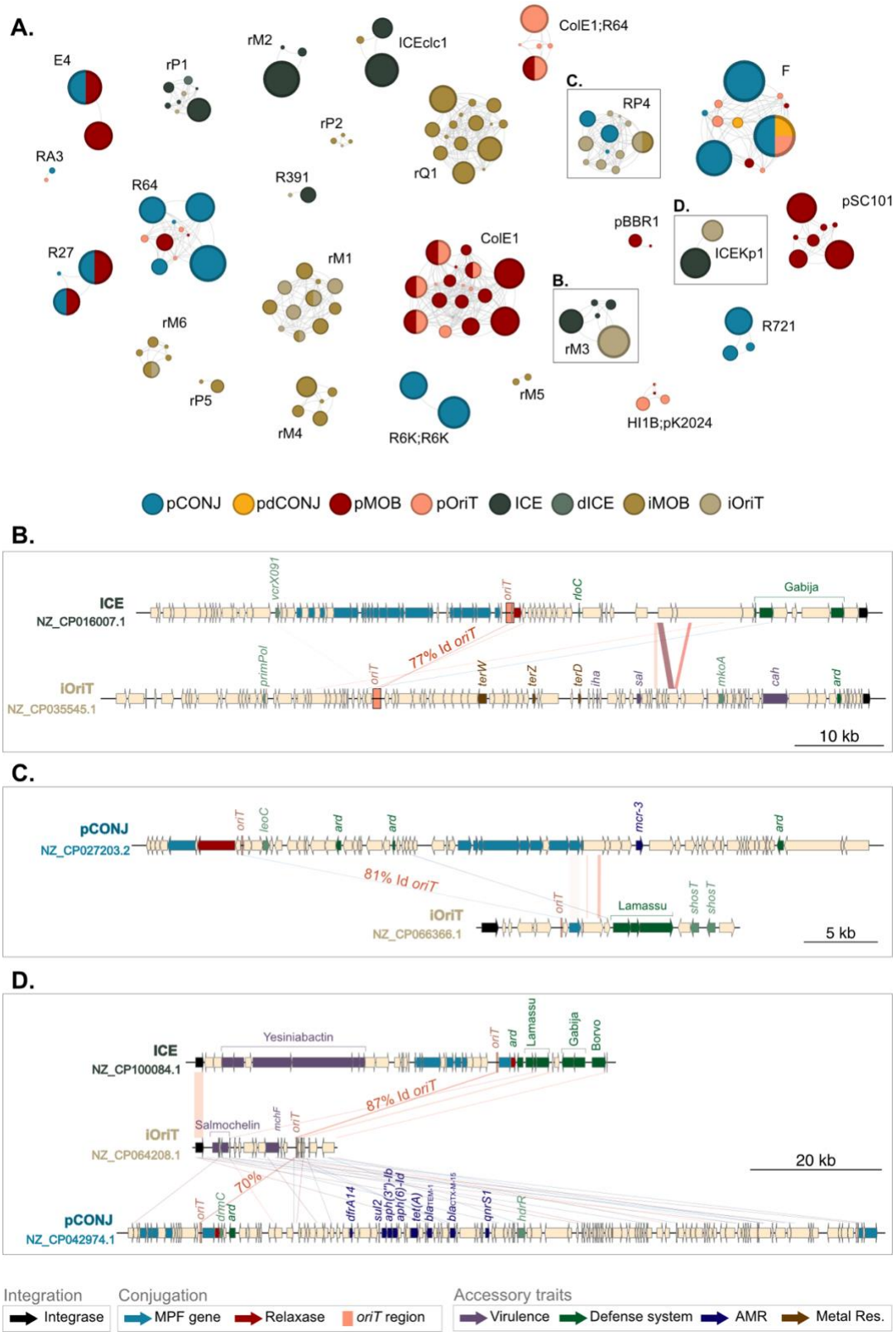

356

357 **Figure 5. A.** MGE communities carrying the same *oriT* families. Nodes represent communities, their size
358 indicating the community size (number of elements) and color indicating the dominant MGE (>75% of the

359 community). When more than one color is shown, it indicates two frequent MGEs. Nodes are connected when
360 communities carry the same *oriT* family, its name being indicated next to the cluster. The three grey squares
361 highlight the communities further detailed in B., C., and D., respectively. **B-D.** Sequence alignment of elements
362 carrying the *oriT* families $oriT_{rM3}$, $oriT_{RP4}$ and $oriT_{ICEKp1}$, respectively. The arrows indicate genes and their colors
363 the functional groups (legend at the bottom).
364

365 ## iOriTs provide critical traits to their hosts

366 Given the diversity of sizes and gene repertoires of iOriT (Fig 5B-D), we assessed their potential
367 functional contribution to bacterial adaptation. As is typical of MGEs, the most common categories
368 are unknown functions (S) or replication-recombination (L) (Fig S16). However, iOriTs were enriched
369 in specific categories compared to other elements, such as signal transduction mechanisms (T) or
370 amino acid metabolism (E). We then focused on specific functions often associated with genomic
371 islands in the literature[28], including virulence factors, antibiotic resistance genes, and anti-MGE
372 defense systems (Fig 6A). These functional repertoires vary across types of MGEs, with the density of
373 virulence factors being higher in iOriT than in any other types of integrative elements or plasmids (Fig
374 6A, Fig S17). Defense systems are present in all MGEs, while counter-defense tend to be less frequent
375 in iOriTs (Fig S16). While antimicrobial resistance is very frequent in pOriT[6], it is almost absent from
376 integrative IMEs (Fig 6A). This is intriguing as some iOriT carry $oriT_{ICEKp1}$ that are also carried by plasmids
377 with antimicrobial resistance genes (Fig 5C). In contrast, many iOriT encode tellurite resistance, which
378 is their only common resistance trait (Fig 6D). The reasons for these differences are intriguing and
379 suggest that iOriT impact some processes (virulence, defense, metal resistance) more than others
380 (antibiotic resistance).

381 We identified many MGE-defense and antidefense genes in iOriTs (5.01 genes/100Kb), in agreement
382 with recent studies in other MGEs[59]. Among these, genes encoding anti-restriction enzymes,
383 restriction-modification systems, and orphan methylases are the most common (Fig 6B). Anti-
384 restriction proteins were found on large iOriTs and are nearly absent in smaller elements (Fig S18).
385 Similar trends were observed in plasmids and could be explained by smaller elements bypassing
386 restriction barriers without the need of expressing anti-restriction[60]. Anti-MGE systems frequent in
387 iOriT include Lamassu-like systems, which were proposed to contribute to the rarity of plasmids in the
388 7th pandemic *V. cholerae* strains[61]. Lamassu is the 3rd most common complete defense system in iOriTs,
389 with more than 500 occurrences across ICE, dICEs, and iMOBs. Remarkably, we found 956 genes
390 predicted as being part of defense systems but lacking the remaining genes. They are often co-
391 localized with unknown function genes or other complete defense systems (Fig 6C), suggesting they
392 could be novel defense systems (or variants of known ones). Most defense systems found in iOriTs
393 and other ICEs and IMEs were located close to the origin of transfer (Fig 6D-E, Fig S19, see Methods).
394 Next to the *oriT* lies the leading sequence that first enters the recipient cell during conjugation[62]. It

395 was recently shown that leading sequences of conjugative plasmids contain multiple anti-defense
396 systems allowing the plasmid to counteract the recipient cell defense systems[63]. These results suggest
397 that integrative elements transferring by conjugation also use anti-defense and defense systems in
398 leading sequences to increase their chances of successful transfer.

399 Strikingly, many iOriTs encode virulence factors, having a much higher density of these genes (3.47
400 genes/100Kb) than ICEs. The iOriT communities include known Pathogenicity Islands (Fig 6F). For
401 instance, the large family of iOriT with $oriT_{M5/6}$ previously identified as TAI islands encode the virulence
402 *iha* gene which encodes for an adhesin important in urinary tract infections (Fig 5B)[55]. The community
403 of small iOriTs carrying the $oriT_{ICEKp1}$ (previously identified as GIE492) encodes the microcin and
404 salmochelin genes associated to hypervirulent *K. pneumoniae* (Fig 6G)[64]. Crucially, they have *oriTs*
405 similar to those of the known pathogenicity island ICE*kp1* and often co-occur in the same genomes
406 (Fig S20), suggesting that elements of different type may be co-mobilized together to provide a larger
407 array of virulence factors to pathogenic bacteria.

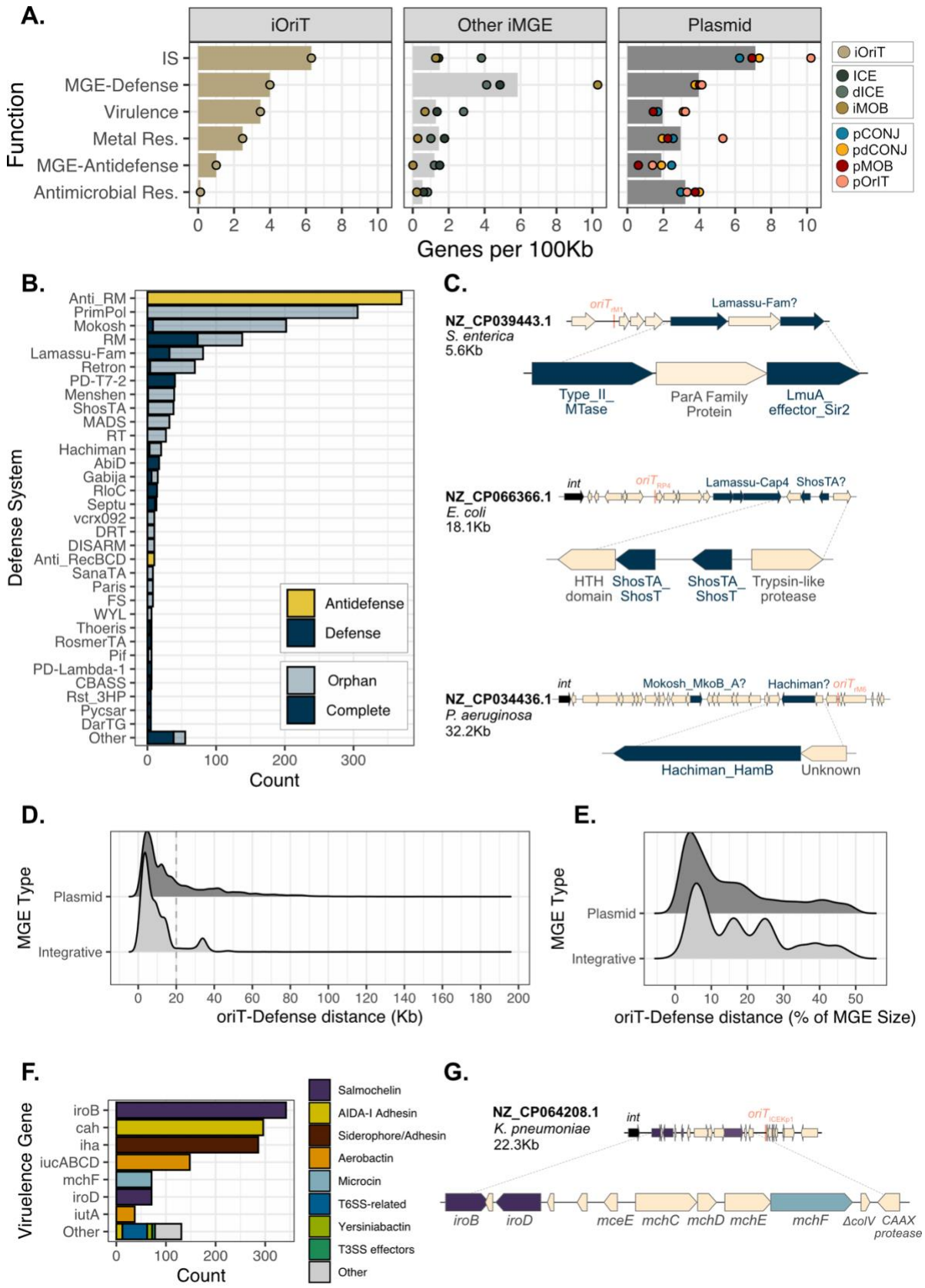

Figure 6. A. Gene density (gene number per 100Kb) of selected traits/functions encoded in iOriTs (left), other integrative MGEs (center), and plasmids (right). The colored dots indicate the gene density for each MGE type. **B.** Most common defense systems (blue) and antidefense genes (yellow) identified across iOriTs. Orphan genes (genes identified in the absence of a complete system) are shown in a lighter blue. **C.** Three cases of orphan genes in iOriTs. In each case, the full iOriT is represented next to the accession number of its genome, species,

414 and size (upper part), and the location and annotation of its defense and adjacent genes (bottom). **D.**
415 Distribution of the absolute distance (Kb) between every defense system and anti-defense gene and the origin
416 of transfer. **E.** Distribution of the distance between the defense and anti-defense systems compared to the MGE
417 size (percentage of its genome size). **F.** Most common virulence genes identified across iOriTs. **G.** Genetic map
418 of an iOriT with the $oriT_{ICEKp1}$. The virulence genes are highlighted, their color matching the legend of panel D.
419

420 ## DISCUSSION

421 Bacteria harbor a plethora of Genomic Islands acquired by Horizontal Gene Transfer, but whose
422 mobility mechanisms remain elusive. Here, we further developed our method to identify novel *oriT*
423 families to find thousands of integrative elements mobilizable by conjugation, including over 1,500
424 putative iOriTs. This suggests that many GIs can be mobilized by conjugation via *oriT* mimicry. We have
425 reasons to believe this large number of integrative hitchers is still an underestimate. Even if we could
426 identify *oriT*s in almost all ICEs, we may have failed to identify some *oriTs,* especially those encoded
427 far from the relaxases or near previously unrecognized relaxases. The latter should not be
428 underestimated, as revealed by our observation that numerous MOB_M relaxases were previously
429 undetected among some of the best studied bacteria. Lastly, hitchers may use mechanisms that we
430 have not studied here. For example, MGIVchHai6 uses a relaxosome accessory protein (MobI) to
431 exploit conjugative plasmids by modifying the affinity of their relaxases, thereby having a different
432 *oriT* from the ones contiguous to the helper's relaxase[65]. Some hitchers integrate in or next to ICEs[66],
433 or in conjugative plasmids[67], to transfer by conduction, which dispenses them from encoding an *oriT*.
434 Some IMEs integrate ICEs and their excision is necessary to the transfer of both elements[68]. They
435 produce complex integrative elements that may be difficult to disentangle without dedicated
436 experimental studies. Finally, ICEs may conjugate before excision from the chromosome, thereby
437 transferring neighboring chromosomal sequences and MGEs[50,69,70]. Here, we showed that some iOriTs
438 are previously identified Pathogenicity or Defense Islands whose mechanisms of mobility remained
439 unknown, sometimes decades after their discovery. Further work is likely to reveal an even greater
440 number of conjugative hitchers.
441
442 This work reveals that integrative elements mobilizable by conjugation are much more abundant than
443 ICEs (Fig 3A). Previous works showed fewer differences[14,16], which is explained by the identification of
444 the iOriT that is novel to this work and by more sensitive identification of the very abundant MOB_M
445 relaxases. A large excess of integrative hitchers relative to conjugative helpers was also previously
446 observed in plasmids[8]. Together, these works show that most elements being mobilized by
447 conjugation are not autonomous and require the help of a conjugative element.
448

449 Intriguingly, the frequency of each type of MGE largely depends on the species: integrative MGEs
450 largely outnumber plasmids in *P. aeruginosa, S. enterica* and *V. cholerae* and are clearly outnumbered
451 by the latter in the other three species (Fig 3B). This wide variation could partly be explained by the
452 presence of specific anti-MGE systems, like Lamassu. While only a few specifically anti-plasmid
453 systems have been uncovered[61,71,72], the current focus on anti-phage systems may have hidden a
454 larger diversity of mechanisms that could be present among the many chimerical or putatively partial
455 defense systems uncovered by ours and others analyses (Fig 6BC). Anti-plasmid systems encoded by
456 integrative MGEs may thus directly contribute to the rarity of plasmids in some genetic backgrounds.
457 In addition, intrinsic properties of the two different types of elements may contribute to the observed
458 differences in their frequency. For example, it was proposed that conjugative plasmids tend to evolve
459 faster in terms of gene repertoires, whereas ICEs may be more stable and have broader host range[46].
460 It would be important to test if such differences also apply to their hitchers.
461
462 The identification of *att* sites in many elements allowed for the first time to systematically query the
463 size and gene repertoires of integrative elements at a large scale. While our methods differ, we found
464 an excellent concordance with the much broader data on Genomic Islands by TIGER[47], which did not
465 specifically searched to characterize hitchers. The clustering of integrative elements revealed clearly
466 separated groups that tend to be homogeneous in terms of genetic mobility, i.e. that are dominated
467 by one type (like the iOriT groups in Fig 5). This suggests that differentiation between elements
468 transferred by conjugation is ancient, although transitions between types mediated by deletions can
469 be observed. Recently, there have been attempts to class plasmids using genetic similarity into groups,
470 notably in Plasmid Taxonomic Units[73]. Our results now suggest that such methods might be used with
471 equal success to class integrative elements. Since MGEs often cross the boundaries of our definitions[42],
472 we propose to call them Conjugative Taxonomic Units by analogy. As a rule, our results show that
473 within a group all or most elements have the same *oriT* family.
474
475 Hitchers are expected to exploit helpers with *oriT*s of the same family, even though we cannot know
476 at this stage if a hitcher can exploit many or just a few of the potential helpers carrying the same type
477 of *oriT*. Nevertheless, an intriguing finding of our work is the specificity of MGEs relying on *oriT*
478 mimicry: plasmid hitchers tend to exploit conjugative plasmids, while integrative hitchers tend to
479 exploit ICEs (Fig 4). This specificity should not derive from fundamental differences in the conjugation
480 mechanisms, which are very similar and share a long evolutionary history[13,74]. Instead, the reasons of
481 this specificity could be explained by the processes of emergence of hitchers. Firstly, hitchers may
482 evolve from helpers by total or partial loss of the MPF locus, as previously found in plasmids [49]. This

483 results in hitchers and helpers having similar *oriT*s. This is consistent with the observation of 21 iOriTs
484 in communities dominated by other types of elements. Secondly, functional dependencies between
485 integrative and plasmid elements may require additional layers of genetic regulation. Conjugation of
486 integrative elements requires the previous excision and circularization of the element to avoid
487 conjugation of large fractions of the bacterial chromosome[75,76]. An IME acquiring an *oriT* from a
488 conjugative plasmid would thus be at the risk of constantly conjugating the chromosome. Accordingly,
489 excision and conjugation were found to be tightly regulated in ICEs and IMEs[77–80]. Some hitchers do
490 not follow this rule. The iOriTs carrying an origin of transfer similar to that of the conjugative plasmid
491 RP4 form large communities across several species suggesting they are ancient iOriTs with gene
492 repertoires unrelated to those of RP4-like plasmids. Indeed, a parallel study has simultaneously
493 revealed the presence of these IMEs carrying $oriT_{RP4}$ across 100 species of Pseudomonodota[57]. These
494 prevalent integrative elements seem to have evolved the ability to hijack these conjugative plasmids
495 *de novo*, e.g. by acquiring the *oriT* by genetic exchanges. Exchanges between different types of MGEs,
496 including ICEs and plasmids, have described numerous times[81,82] and could also contribute to the
497 emergence of hitchers.
498
499 Conjugation can transfer huge amounts of DNA in one event, up to a complete genome[83], contrary to
500 other mechanisms like transduction[84,85]. Yet, there are very specific size distributions for these
501 elements: ICEs tend to be large, iMOBs small, and the distribution of sizes of iOriT is bimodal.
502 Analogous plasmids follow similar distributions, with the difference that pMOB plasmids are also
503 largely bimodal[6]. The differences in size between ICEs and IMEs was previously identified and is likely
504 due to the requirement of encoding a MPF which can require from 11 to dozens of genes[36]. While
505 plasmids and integrative elements have approximately the same average size, their ranges of variation
506 are different. The smallest IMEs are larger than the smallest mobilizable plasmids, possibly because of
507 the sequence required to encode the integration genetic module and its regulatory components.
508 Indeed, while more than 1,200 plasmids (11.5%) encode less than 5 genes, only 12 IMEs (0.5%) were
509 in the same situation (Fig S21). At the other edge of the distribution, while large ICEs have been
510 described (e.g. the 800 kb tri-partite ICE[22]) there are many more very large plasmids in our dataset.
511 Larger integrative elements might be costly by disrupting chromosomal organization. In the other side,
512 smaller integrative elements might result from gene deletion *in situ*, as observed by the higher number
513 of decaying elements in chromosomes (dICEs) compared to plasmids (pdCONJ) (Fig 1E). Decaying
514 pdCONJ are rapidly lost[49]. In contrast, dICEs are not affected by the segregationally loss imposed to
515 plasmids and may remain in genomes for longer periods of time.
516

517 An intriguing observation of this study is that among elements mobilizable by conjugation, those that
518 integrate the chromosome encode traits very different from those that are plasmids. While pOriT are
519 enriched in antimicrobial resistance, IMEs are enriched in MGE-defense systems, and iOriTs are
520 specifically enriched in virulence factors. Antimicrobial resistance has been associated to conjugative,
521 fast evolving plasmids[86], while ICEs were proposed to be less plastic[46]. This might explain the
522 differences we observe. Of note, integrative elements have been associated to AMR in other
523 species[16,87], and it's possible that such differences are species specific. In contrast, iOriT encode many
524 anti-MGE systems and a high density of virulence factors. This raises an interesting parallel between
525 MGEs mobilized by conjugation and temperate phages, whose integrative elements (prophages) and
526 their hitchers (phage satellites) also often encode virulence factors and defense systems, and rarely
527 encode antibiotic resistance[59,88], whereas phage-plasmids encode more frequently antibiotic
528 resistance[89]. Further work is needed to understand these striking, but poorly understood, associations
529 between the mechanisms of vertical and horizontal transmission of MGEs and the accessory traits
530 they encode.

531 MATERIALS AND METHODS

532 **Genome data.** We retrieved the 32,799 complete bacterial genomes from the NCBI non-redundant
533 RefSeq database (https://ftp.ncbi.nlm.nih.gov/genomes/refseq/, accession in May 2023). Only the
534 6,182 genomes belonging to *Escherichia coli* (n=2,559), *Salmonella enterica* (n=1,293), *Klebsiella*
535 *pneumoniae* (n=1,522), *Vibrio cholerae* (n=107), *Neisseria gonorrhoeae* (n=142), and *Pseudomonas*
536 *aeruginosa* (n=559), were selected for further analysis. These genomes had one or two chromosomes
537 (*V. cholerae*) and 13,090 plasmids: *Escherichia coli* (n=6,135), *Salmonella enterica* (n=1,465), *Klebsiella*
538 *pneumoniae* (n=5,154), *Vibrio cholerae* (n=16), *Neisseria gonorrhoeae* (n=166), and *Pseudomonas*
539 *aeruginosa* (n=154). Accession numbers of genomes can be found in Table S2.

540 **Functional annotation.** Genomes were annotated using Prodigal v2-6-3, with the option *-p meta*,
541 recommended for mobile genetic elements[90]. The COG categories of the proteins were inferred using
542 the software eggNOG-mapper, version 2.1.12[91]. We used the module CONJscan of MacSyFinder,
543 version 2.0 to identify protein coding genes related to conjugation, such as relaxases and the MPF
544 systems[92]. MGE defense systems were screened using DefenseFinder, v1.3.0, retrieving both complete
545 systems and orphan hits using the option *--preserve-raw* [93]. Antidefense systems were also screened
546 using the option *–antidefensefinder*[94]. Genes related to antimicrobial resistance, heavy metal
547 resistance, stress response, and virulence were identified with AMRFinderPlus, version 3.11.4[95].
548 Virulence genes were additionally screened using BLASTp of BLAST 2.9.0+[96], using as query the 27,982

549 protein sequences available in the virulence factor database VFDB (http://www.mgc.ac.cn/VFs/,
550 accession in August 2024)[97], retrieving only the hits >50% identity and >50% coverage. Insertion
551 Sequences were screened using ISEScan, version 1.7.3[98], with default parameters. Integrases were
552 identified screening the PFAM domains for tyrosine recombinases (PF00589.27) and serine
553 recombinases (PF00239.26 and PF07508.18), with a coverage >40%[99]. For serine recombinases, only
554 proteins containing both domains were considered.

555 **Identification of occurrences of origins of transfer of known families.** *oriTs* of known families were
556 retrieved from three different collections: an in-house collection of 96 experimentally validated *oriTs*
557 from the literature[6]; a collection of 122 experimentally validated *oriTs* available in the updated
558 database oriTDB[100]; and 21 *oriT*-comprising regions recently inferred from *E. coli*, *K. pneumoniae* and
559 *Acinetobacter baumannii*, six of which were experimentally validated[35]. To note, an updated sequence
560 of the region $oriT_{FK}$ and extended versions of $oriT_{CloDF13}$[101] and $oriT_{pAD1}$[102] are provided. After removing
561 redundant *oriTs* across the collections, we obtained a final dataset of 168 non-redundant known *oriTs*
562 and *oriT*-comprising regions (Dataset S1). Known *oriTs* were clustered by sequence similarity into *oriT*
563 families. This was done using the Smith-Waterman algorithm of the FASTA package, v36.3.8i
564 (ssearch36, E-value<0.001)[103]. The parameter we used for the clustering is the alignment bitscore since
565 it is independent of the database size and directly reflects the sequence similarity and alignment
566 length. However, the bitscore depends on the pair of aligned sequences, and cannot be used directly
567 to compare different alignments. Instead, it can be normalized in a value between 0 and 1 by
568 comparing how well two sequences align to each other, relative to how well they align to themselves
569 (i.e., the maximum bitscore for that particular pair). This ensures a length-independent, symmetric,
570 and comparable normalized bitscore. To do so, we employed the following formula:

571 $$bs_{norm} = \frac{bs_{qt} + bs_{tq}}{bs_{qq} + bs_{tt}}$$

572 where bs_{norm} is the normalised bitscore; bs_{qt} is the bitscore of the alignment query vs. target; bs_{tq} from
573 target vs. query; bs_{qq}, query vs. query; and bs_{tt}, target vs. target. The bs_{norm} was used for hierarchical
574 clustering analysis of the non-coding sequences using the Ward.D2 method of the R package
575 pheatmap (v.1.0.12) (https://CRAN.R-project.org/package=pheatmap). The 168 *oriTs* were grouped
576 into 90 *oriT* families, named after well-known *oriTs* they contain (Table S3). For instance, the family
577 $oriT_{F}$ includes ten non-redundant *oriTs* from the three sources: $oriT_{F}$, $oriT_{ColB4}$, $oriT_{P307}$, $oriT_{pSU233}$, $oriT_{R1}$,
578 and $oriT_{R100}$ of our in-house collection; $oriT_{F}$, $oriT_{pEC156\_1}$, and $oriT_{pKPHS2}$ of the oriTDB; and the $oriT_{FK}$
579 containing region. Known *oriT* families were screened using BLASTn of BLAST 2.9.0+ [96], with the

580 options *-task blastn-short -evalue 0.01*. Only the hits with an identity >50% and coverage >50% were
581 retrieved.

582 **Identification of previously uncharacterized origins of transfer.** To identify unknown *oriT*-comprising
583 regions across the complete genomes, we used a method recently described for plasmids[35]. Briefly,
584 we retrieved the first intergenic sequence >50nt upstream the relaxase genes of both chromosomes
585 and plasmids. Among the 14,429 sequences, redundant sequences were identified clustering by
586 sequence similarity using MMSeqs2, version 13.451[104], with a criterion of 100% identity and 100%
587 coverage. Only one representative per cluster was randomly picked for subsequent analysis. This
588 resulted in a dataset of 3,111 non-redundant intergenic sequences upstream a relaxase that were split
589 into seven groups according to their MOB family: 242 MOB_C, 373 MOB_F, 461 MOB_H, 186 MOB_M, 1255
590 MOB_{P1}, 408 MOB_Q and 70 MOB_V. Per group, we performed an all-vs-all local alignment of the
591 intergenic sequences using the Smith-Waterman algorithm of the FASTA package, v36.3.8i (command
592 ssearch36)[103], retrieving only the hits with an E-value <0.001, identity >50%, coverage >30%, alignment
593 length >50 nt.

594 The results were used to cluster the sequences using the Ward.D2 method of the R package pheatmap,
595 version 1.0.12 (https://CRAN.R-project.org/package=pheatmap), based on the normalized bitscore
596 (see above). This clustering was performed for each MOB family independently. Hierarchical clustering
597 may encounter difficulties when aiming at unveiling small clusters in the presence of large ones. To
598 tackle this limitation, we performed the clusters in serial rounds. For instance, in case of MOB_{P1}, we
599 clustered the 1,255 sequences into the 17 largest clusters (average 57 sequences per cluster), leaving
600 the remaining 288 sequences as an outgroup. In a second round, the outgroup was clustered into 57
601 clusters (4 per cluster). Small clusters (<5 sequences/cluster) were discarded, resulting in a total
602 number of 36 clusters. Each cluster represents a candidate *oriT*-comprising region for MOB_{P1}. The
603 same procedure was followed for each MOB group, resulting in 212 clusters (2,417 sequences). Among
604 these *oriT*-comprising regions, 29 were discarded since they belong to plasmids where the *oriT* is not
605 located upstream to the MOB (e.g., $oriT_F$, $oriT_{pVCR94X}$).

606 We performed different validations with the remaining 183 clusters. First, a multiple sequence
607 alignment (MSA) was performed to validate the quality of the clusters. We used mafft, version v7.505,
608 with the options *--maxiterate 1000 –genafpair*[105]. The MSAs were then examined with the software
609 SnapGene, version 7.0.3 (www.snapgene.com), and 11 clusters were discarded due to the bad quality
610 of the MSA. Second, we examined the genetic location and surrounding areas of the sequences using
611 SnapGene, version 7.0.3 (www.snapgene.com). Among them, 41 clusters were discarded due to either
612 gene rearrangements (e.g., Insertion Sequences upstream the relaxases), or wrong annotations (e.g.,

613 the first intergenic sequence was not properly annotated). Among the 131 remaining clusters, some
614 were grouped into the same *oriT* family since their sequences contained the same known *oriT* (*e.g.*,
615 $oriT_{R46}$ was identified across the sequences of two clusters), finally reaching 115 clusters. After the first
616 screening (see below), these 115 *oriT*-comprising regions had recognizable instances in the 87% of the
617 relaxase-carrying Genomic Islands. For the sake of completeness, we repeated the same pipeline with
618 the relaxases lacking *oriTs* without removing redundant intergenic sequence prior to the hierarchical
619 clustering. The analysis resulted in 9 additional clusters, leaving only 7% of the relaxases without a
620 putative *oriT*.

621 These 124 *oriT*-comprising regions were clustered, together with the previously known *oriTs*, by
622 sequence similarity into *oriT* families, as previously explained. This resulted in a total of 76 families of
623 origins of transfer, of which 52 are new. Novel *oriT* family regions were named according to their MOB
624 associated and a numeric identifier. To distinguish these *oriT*-comprising regions from delimited *oriT*
625 sequences, an '*r*' standing for '*region*' was added to the name. Therefore, the families rQ1 ($oriT_{rQ1}$)
626 and rQ2 ($oriT_{rQ2}$) correspond to two different *oriT*-comprising regions associated to MOB_Q relaxases.

627 **Identification of *oriTs* distant to the relaxases**. Since the HMM profiles used to screen for *oriTs* were
628 built using the clustering of intergenic sequences upstream relaxases, our approach misses those few
629 *oriTs* known to be located far from the relaxase: $oriT_F$[3], $oriT_{pVCR94X}$[106], $oriT_{R391}$[107], $oriT_{ICEclc2}$[45], $oriT_{pK2044}$[108].
630 So, we retrieved all the blastn hits obtained from each of these queries (as previously explained in
631 'Screening of known origins of transfer') with the tools from SeqKit, version 2.8.2[109], to perform a MSA
632 using mafft version v7.505[105] and build HMM profiles using HMMER, version 3.3.2[110].

633 **Screening of the uncharacterized *oriTs* across the complete genomes**. To screen for the candidate
634 *oriT*-comprising region across the complete genomes, we used the MSAs previously performed to
635 build Hidden-Markov model (HMM) profiles of each of the clusters. First, the MSAs were manually
636 trimmed in SnapGene, version 7.0.3 (www.snapgene.com). The edges were removed, keeping the
637 alignment from the first ten consecutive nucleotides in a row within the consensus sequence to the
638 last ten consecutive nucleotides in a row within the consensus sequence. Additionally, every sequence
639 whose length was <50% or >50% of the consensus sequence of the trimmed MSA was discarded. In
640 cases where an already known *oriT* was identified in the *oriT* regions, the former was included in the
641 MSA, and the trimming was performed from the beginning to the end of the experimentally validated
642 origin of transfer. The trimmed MSAs were then used to build HMM profiles employing the command
643 hmmbuild of HMMER, version 3.3.2[110]. Once the HMM profiles were built, we used nhmmscan to
644 screen for the *oriTs* and *oriT*-comprising sequences across the 6,182 complete genomes.

645 **Validation of the *oriT* diversity within the species.** To assess if the novel *oriTs* inferred in this work
646 cover the *oriT* diversity within the species, we retrieved a supplementary dataset including the 2,289
647 genomes of the six species submitted between June 2023 and May 2025
648 (https://ftp.ncbi.nlm.nih.gov/genomes/refseq/, accession in June 2025). The genomes were screened
649 for relaxases and *oriTs* as previously described.

650 **Identification of defense and anti-defense systems in the conjugative leading region.** Defense/anti-
651 defense systems were searched in the first DNA region to enter the cell during conjugation (i.e, the
652 conjugative leading region), defined in plasmids as the one adjacent to the *oriT* in the opposite
653 direction to the relaxase and/or relaxosome accessory protein genes (Fig S19A)[2,3,63]. Most conjugative
654 plasmids in these species carry a MOB_{P1} or MOB_F with the *oriT* locating at one side of the relaxase-
655 MPF module (Fig S19B)[3]. In these cases, the leading region is in accordance with the previous
656 definition. However, that in many integrative elements, such as definition was not necessarily
657 warranted. The conjugative machineries with MOB_C or MOB_M, which are the most abundant in ICEs
658 (and also present in plasmids, see below), harbor the *oriT* between the MPF operon and the relaxase
659 gene (Fig S19C)[58]. Even more complex scenarios arise with MOB_H systems, where the *oriT*, relaxase,
660 and different modules of the MPF system are encoded in different regions of plasmids[111,112], thereby
661 complicating the *in silico* identification of the leading region (Fig S19C). Given the diversity of such
662 cases and in lack of experimental data for these elements, we computed the absolute distance
663 between the *oriT* and every anti-defense gene and defense system identified with DefenseFinder
664 v1.3.0[94]. Only elements with one *oriT* were considered for the analysis.

665 **Classification of Mobile Genetic Elements.** Integrative MGEs were classified according to their
666 mobility, following the most recent classification of plasmids (Fig 1A)[42]. Briefly, MGEs encoding a
667 relaxase and a complete MPF system were classified as Integrative Conjugative Elements (ICEs) when
668 integrated in the chromosome, or conjugative plasmids (pCONJ) when episomal. MGEs encoding an
669 incomplete MPF system, with or without a relaxase, were considered decayed ICEs (dICEs) or decayed
670 pCONJ (pdCONJ). Integrative elements missing a MPF system were classed as Integrative Mobilizable
671 Elements (IMEs) and could carry their own relaxase (iMOB) or only an *oriT* (iOriT). Likewise, plasmids
672 carrying an *oriT*, with or without a relaxase gene, were classed as mobilizable plasmids (pMOB and
673 pOriT, respectively). Plasmids with phage-like functions characteristic of phage-plasmids were
674 identified using the tyPPing pipeline[113]. The remaining plasmids were considered non-transmissible
675 (pNTs). Plasmids were assigned to a Plasmid Taxonomic Unit (PTU) when possible, using COPLA,
676 version 1.0[114]. By using the module CONJscan of MacSyfinder, version 2.0[92], plasmids, ICEs and IMEs
677 encoding a relaxase were assigned to one of the nine MOB classes encompassing the phylogenetic

678 diversity of relaxases[115]: related to HUH-endonucleases (MOB_B, MOB_F, MOB_P, MOB_Q, MOB_V), HD-
679 hydrolases (MOB_H), restriction endonucleases (MOB_C), rolling-circle replicases (MOB_T), or related to
680 tyrosine recombinases (MOB_M). Also, elements carrying a complete or incomplete MPF system where
681 assigned to one of the eight MPF monophyletic groups[13]: MPF_I, MPF_C, MPF_G, MPF_T, MPF_F, MPF_B, MPF_{FA},
682 or MPF_{FATA}. Detailed information on the plasmids and integrative elements is available in
683 Supplementary Tables S4-S6.

684 **Identification of MOB_M relaxases.** Over the course of the project, we realized that the state-of-the-
685 art methods to identify relaxases missed occurrences of the MOB_M family (not to be confused with
686 the MobM protein of pMV158, which is MOB_V family[116]). Just three occurrences of the relaxase have
687 been described in the literature: TcpM in the conjugative plasmid pCW3 of *Clostridium*
688 (ABC96296.1)[40], MobK in the mobilizable plasmid pIGRK of *Klebsiella* (AAS55463.1) [39], and MpsA in the
689 IME SGI1 of *Salmonella* (AAK02039.1)[37]. The screening for MOB_M proteins in the available software
690 relies on a HMM profile based on the *Clostridium* pCW3 relaxase and it overlooks phylogenetically
691 distant MOB_M. Given the species composition of our database, we built a new HMM profile for their
692 identification.

693 First, we identified MOB_M in our dataset using two rounds of BLASTp of BLAST 2.9.0+[96]. The first round
694 used seven relaxases as query - the three known MOB_M, and four other instances identified in our
695 dataset (WP_033567157.1, WP_047656026.1, WP_001096463.1, WP_004252296.1). Only the hits
696 with an E-value <0.001 and coverage >30% were retrieved. The 1,156 proteins identified in the first
697 round were then used as query in a second BLASTp, retrieving 1,521 hits with an E-value <0.001,
698 identity >30%, and coverage >50%. Across the latter proteins, identical sequences were deduplicated
699 using MMSeqs2, v.13.4511[104]. The 143 deduplicated MOB_M sequences were aligned using MAFFT,
700 version 7.505, options *--maxiterate 1000 –genafpair*[105]. The MSA was trimmed from the edges and
701 used to build an HMM profile using hmmbuild from HMMER, v3.3.2[110] (Dataset S2). Lastly, the HMM
702 profile was used to screen for MOB_M relaxases across the dataset using hmmsearch and retrieving hits
703 with an E-value <0.001. MOB_M relaxases are closely related to tyrosine recombinases[39]. Therefore, to
704 avoid false positive results with these proteins, we set a score *cut_ga* of 84, which allows the
705 identification of MOB_M relaxases while discarding tyrosine recombinases.

706 **Identification of interval-delimited Genomic Islands (GI^{id}) across bacterial chromosomes**. The
707 genomic location of the MGEs were placed in relation to the location of persistent genes in each
708 species to facilitate MGE delimitation and to compare locations across distinct genomes. For this, we
709 computed the pangenome of each species using the pangenome module of Panacota, v1.4.1-dev3[117],
710 applying a minimum sequence identity threshold of 80% and a coverage threshold of 80%. We

711 extracted from the pangenome the persistent gene families, i.e., those present in single copy in at
712 least 90% of the genomes of the species using the module corepers of PanACoTA, v1.4.1-dev3[117]. We
713 then defined *intervals* as the regions between two consecutive persistent genes in genomes. By
714 definition, MGEs are not part of the persistent genome in most species. Hence, integrative MGEs are
715 absent from persistent genes and constrained within intervals, providing upper bound to the position
716 of the integrative MGES. We therefore defined interval-delimited Genomic Islands (GI^{id}) as the interval
717 where the MGE is present.

718 **Identification of genomic spots.** Intervals from genomes of the same species were grouped in
719 genomic spots when they are flanked by the same pair of persistent gene families, allowing
720 comparison of equivalent regions across genomes. The number of genetic spots occupied by ICE/IMEs
721 was generally low in the species (from 3 spots in *Ng* to 72 in *Pa*). Some intervals are flanked by unusual
722 pairs of persistent genes, i.e. pairs that are rarely contiguous in the species. These usually result from
723 the loss of one or both persistent genes or from the action of chromosomal rearrangements. These
724 unusual configurations make the spot assignment ambiguous and MGEs in these regions were often
725 subject to structural changes. Therefore, these intervals were excluded from the analysis (9% of all
726 intervals).

727 **Identification of *att* sites and definition of *att*-delimited Genomic Islands.** Since most ICE and IME
728 integrate the chromosome using a Tyrosine recombinase, we used this information to propose a finer
729 delimitation of the integrative elements. Integration sites were defined as follows: *attB* is the host
730 attachment site prior to MGE integration (ancestral, MGE-free sequence), while *attL* and *attR* are the
731 corresponding sites at the left and right boundaries of the integrated MGE. The latter share sequence
732 similarity since a part of *attB* is duplicated and repeated at the edges of the MGE upon integration[118].
733 This allows their identification by searching for nucleotide sequence similarity within the spot. For
734 each spot, we extracted the shortest interval (in bp) and assumed it represents the ancestral state
735 containing the *attB* site (MGE-free) (Fig S9A). When this assumption does not hold we cannot identify
736 the *att* sites. This interval was then compared with each longer interval containing an MGE. The longer
737 intervals are expected to harbor short DNA repeats of the *attB* sites at the edges of the element, the
738 *attL* and *attR* sites. To ensure at least two significant alignments per comparison enhancing detection
739 reliability, all intervals were extracted including the persistent genes flanking them. To note, all
740 intervals were oriented so that the flanking persistent genes are in the same direction, allowing to
741 restrict the sequence similarity search to the positive strand. This improves computational efficiency
742 and simplifies the identification of overlapping regions. Sequence similarity between the shortest
743 interval containing the *attB* site (query) and each larger interval within the same spot containing

744 candidate *attL*/*attR* (subject) was screened with BLASTn[96], with the options *-evalue 0.001 -strand plus*.
745 Alignments with ≥80% nucleotide identity were retained, and redundant hits fully contained within
746 longer alignments were discarded. Pairs of hits on the subject sequence (large interval) aligning to
747 overlapping regions of the query (short interval) were interpreted as duplication of a sequence
748 segment associated with integration. The overlapping region on the shortest interval was defined as
749 the putative *attB* site. The corresponding regions on the larger interval were defined as *attL* and *attR*
750 sites (Fig S9A). Importantly, this approach makes no assumptions about the genomic context, such as
751 the presence or position of the tyrosine recombinase genes.

752 To search for additional *att*-like sequences in the case of tandem integration events in the same
753 interval (>1 *attL*/*R* per interval), we extracted the previously identified *attL* and *attR* sequences, along
754 with the intergenic genomic region they delimit. Each *attL* and *attR* sequence (>15 bp) was then used
755 as a query in a second BLASTn search against the extracted region to detect additional *att*-like
756 sequences. Due to the short length of the *att* sequences (Fig S9B), BLASTn was run with parameters
757 optimized for short queries *(-task blastn-short -evalue 1e-3 -strand plus*). Only hits with ≥80% identity
758 and an alignment length exceeding 15 bp were retained. In cases of overlapping alignments, only the
759 best-scoring hit was kept to remove redundancy. Retained *att* sites were then ordered according to
760 their genomic coordinates, and *att*-delimited Genomic Intervals (GIs) were defined as the sequences
761 larger than 2 Kb between successive *att* sites. This assumes that integration events occur in tandem
762 relying on the same *att* site[66,119], which is not always the case since some IMEs and other hitchers have
763 been shown to integrate within their helpers[120,121].

764 Most attachment sites are either not experimentally validated or unknown. To provide further
765 evidence of the validity of the *ab initio* identification of *att* sites, we compared the predicted *att* sites
766 with those reported by the TIGER/Islander database[47], restricting the database to the 469,044
767 Genomic Islands identified in the same six species included in our study. Using the original *attL*/*attR*
768 sequences, 99% of sites were recovered, either matching perfectly an *att* site described in the TIGER
769 database or overlapping the sequences flanking the *att* sites (Fig S9C). However, because some *att*
770 sites are very short (average of 21bp in our identification, 9bp in the TIGER database, as short as 2bp),
771 comparisons based solely on their core sequences can yield spurious matches. To address this, each
772 *att* sequence was extended together with its 10 nucleotides upstream and downstream (hereafter
773 "extended *att*"), resulting in longer lengths. The 97% of our extended *att* sites were present in the
774 TIGER database (Fig S9C). All sequences of the *att* sites, as well as the extended *att* sequences are
775 available in Table S1.

776 **Building communities based on the weighted Gene Repertoire Relatedness (wGRR).** To assess the
777 genetic relatedness between MGEs, we calculated the wGRR, using GRIS version 2.0
778 (https://gitlab.pasteur.fr/jgugliel/wgrr) with the default parameters as previously described[46]. Briefly,
779 the software identifies the sequence similarities between all the proteins encoded in the elements
780 using MMseqs2, version 16-747c6[104], and retrieves the best bi-directional hits (BBH) between them.
781 Once the BBHs have been defined, the wGRR can be calculated with the following formula,

782 $$wGRR(A,B) = \frac{\sum_i id(A_i, B_i)}{min(P_A, P_B)}$$

783 where *i* is the number of BBH between the two elements, $id(A_i,B_i)$ is the identity of the BBH, and P_A
784 and P_B are the number of proteins of the elements A and B, respectively. Hence, a wGRR=1 means that
785 the two elements are identical (or one is entirely contained within the other), whereas wGRR=0 means
786 the elements have no homologous protein-coding genes. To build genetically related clusters, we
787 retrieved pairs of elements with wGRR>0.75 and built communities using the Louvain algorithm with
788 the R package igraph, version 1.3.0 (https://CRAN.R-project.org/package=igraph)[122], and the default
789 resolution parameter (N=1). Graphs were visualized using the software Gephi, version 0.10.0[123].

790 ## Data availability

791 The dataset utilized for the current study is publicly available (RefSeq database,
792 https://ftp.ncbi.nlm.nih.gov/genomes/refseq/, accessed in May 2023 and June 2025). The datasets
793 generated are included in this published article and its supplementary information files. HMM profiles
794 of the origins of transfer can be found at figshare[124].

795 ## Code availability

796 Custom R scripts to identify candidate *oriT*-containing regions for this study are available in figshare[125].

797 ## Acknowledgements

798 We thank all the Microbial Evolutionary Genomics Unit members for the regular discussions
799 throughout the project. We also thank F. de la Cruz and M. P. Garcillán Barcia (IBBTEC-Universidad de
800 Cantabria, Spain) for help and advice on this project. This work was funded by the INCEPTION project
801 (PIA/ANR-16-CONV-0005, E.P.C.R.), the Fondation pour la Recherche Médicale (Equipe FRM,
802 EQU201903007835, E.P.C.R.), the ANR LBX-62 IBEID and the ANR EcoRecEp (ANR-23-CE35-0006, M.T.).
803 M.A.A was supported by a Pasteur-Roux-Cantarini fellowship of Institut Pasteur. This work used the

804 computational and storage services (TARS cluster) provided by the IT department at Institut Pasteur,
805 Paris.

806 ## References

807 1. Arnold, B. J., Huang, I.-T. & Hanage, W. P. Horizontal gene transfer and adaptive evolution in bacteria. *Nat*
808 *Rev Microbiol* **20**, 206–218 (2022).
809 2. De La Cruz, F., Frost, L. S., Meyer, R. J. & Zechner, E. L. Conjugative DNA metabolism in Gram-negative
810 bacteria. *FEMS Microbiol Rev* **34**, 18–40 (2010).
811 3. Virolle, C., Goldlust, K., Djermoun, S., Bigot, S. & Lesterlin, C. Plasmid Transfer by Conjugation in Gram-
812 Negative Bacteria: From the Cellular to the Community Level. *Genes* **11**, 1239 (2020).
813 4. Smillie, C., Garcillán-Barcia, M. P., Francia, M. V., Rocha, E. P. C. & de la Cruz, F. Mobility of Plasmids.
814 *Microbiol Mol Biol Rev* **74**, 434–452 (2010).
815 5. Waldor, M. K. Mobilizable genomic islands: going mobile with *oriT* mimicry. *Molecular Microbiology* **78**,
816 537–540 (2010).
817 6. Ares-Arroyo, M., Coluzzi, C. & Rocha, E. P. C. Origins of transfer establish networks of functional
818 dependencies for plasmid transfer by conjugation. *Nucleic Acids Research* **51**, 3001–3016 (2023).
819 7. Lang, A. S., Buchan, A. & Burrus, V. Interactions and evolutionary relationships among bacterial mobile
820 genetic elements. *Nat Rev Microbiol* **23**, 423–438 (2025).
821 8. Ares-Arroyo, M., Coluzzi, C., Moura De Sousa, J. A. & Rocha, E. P. C. Hijackers, hitchhikers, or co-drivers?
822 The mysteries of mobilizable genetic elements. *PLoS Biol* **22**, e3002796 (2024).
823 9. Burrus, V. & Waldor, M. K. Shaping bacterial genomes with integrative and conjugative elements. *Research*
824 *in Microbiology* **155**, 376–386 (2004).
825 10. Johnson, C. M. & Grossman, A. D. Integrative and Conjugative Elements (ICEs): What They Do and How
826 They Work. *Annu. Rev. Genet.* **49**, 577–601 (2015).
827 11. Audrey, B., Cellier, N., White, F., Jacques, P.-É. & Burrus, V. A systematic approach to classify and
828 characterize genomic islands driven by conjugative mobility using protein signatures. *Nucleic Acids*
829 *Research* **51**, 8402–8412 (2023).
830 12. Brochet, M. *et al.* Atypical association of DDE transposition with conjugation specifies a new family of
831 mobile elements. *Molecular Microbiology* **71**, 948–959 (2009).
832 13. Guglielmini, J., de la Cruz, F. & Rocha, E. P. C. Evolution of Conjugation and Type IV Secretion Systems.
833 *Molecular Biology and Evolution* **30**, 315–331 (2013).
834 14. Guglielmini, J., Quintais, L., Garcillán-Barcia, M. P., De La Cruz, F. & Rocha, E. P. C. The Repertoire of ICE in
835 Prokaryotes Underscores the Unity, Diversity, and Ubiquity of Conjugation. *PLoS Genet* **7**, e1002222
836 (2011).
837 15. Guédon, G., Libante, V., Coluzzi, C., Payot, S. & Leblond-Bourget, N. The Obscure World of Integrative and
838 Mobilizable Elements, Highly Widespread Elements that Pirate Bacterial Conjugative Systems. *Genes* **8**,
839 337 (2017).
840 16. Botelho, J. Defense systems are pervasive across chromosomally integrated mobile genetic elements and
841 are inversely correlated to virulence and antimicrobial resistance. *Nucleic Acids Research* **51**, 4385–4397
842 (2023).
843 17. Ramsay, J. P. & Firth, N. Diverse mobilization strategies facilitate transfer of non-conjugative mobile
844 genetic elements. *Current Opinion in Microbiology* **38**, 1–9 (2017).
845 18. Achard, A. & Leclercq, R. Characterization of a Small Mobilizable Transposon, MTnSag1, in *Streptococcus*
846 *agalactiae*. *J Bacteriol* **189**, 4328–4331 (2007).
847 19. Carraro, N., Rivard, N., Ceccarelli, D., Colwell, R. R. & Burrus, V. IncA/C Conjugative Plasmids Mobilize a
848 New Family of Multidrug Resistance Islands in Clinical Vibrio cholerae Non-O1/Non-O139 Isolates from
849 Haiti. *mBio* **7**, e00509-16 (2016).
850 20. Daccord, A., Ceccarelli, D., Rodrigue, S. & Burrus, V. Comparative Analysis of Mobilizable Genomic Islands.
851 *Journal of Bacteriology* **195**, 606–614 (2013).
852 21. Botelho, J. & Schulenburg, H. The Role of Integrative and Conjugative Elements in Antibiotic Resistance
853 Evolution. *Trends in Microbiology* **29**, 8–18 (2021).
854 22. Colombi, E. *et al.* Comparative analysis of integrative and conjugative mobile genetic elements in the
855 genus Mesorhizobium. *Microbial Genomics* **7**, (2021).

23. LeGault, K. N. *et al.* Temporal shifts in antibiotic resistance elements govern phage-pathogen conflicts. *Science* **373**, eabg2166 (2021).
24. Seth-Smith, H. M. B. *et al.* Structure, Diversity, and Mobility of the Salmonella Pathogenicity Island 7 Family of Integrative and Conjugative Elements within Enterobacteriaceae. *J Bacteriol* **194**, 1494–1504 (2012).
25. Jones, J. M., Grinberg, I., Eldar, A. & Grossman, A. D. A mobile genetic element increases bacterial host fitness by manipulating development. *eLife* **10**, e65924 (2021).
26. Bean, E. L., McLellan, L. K. & Grossman, A. D. Activation of the integrative and conjugative element Tn916 causes growth arrest and death of host bacteria. *PLoS Genet* **18**, e1010467 (2022).
27. Reinhard, F., Miyazaki, R., Pradervand, N. & van der Meer, J. R. Cell Differentiation to "Mating Bodies" Induced by an Integrating and Conjugative Element in Free-Living Bacteria. *Current Biology* **23**, 255–259 (2013).
28. Boyd, E. F., Almagro-Moreno, S. & Parent, M. A. Genomic islands are dynamic, ancient integrative elements in bacterial evolution. *Trends in Microbiology* **17**, 47–53 (2009).
29. Juhas, M. *et al.* Genomic islands: tools of bacterial horizontal gene transfer and evolution. *FEMS Microbiol Rev* **33**, 376–393 (2009).
30. Hacker, J. & Kaper, J. B. Pathogenicity Islands and the Evolution of Microbes. *Annu. Rev. Microbiol.* **54**, 641–679 (2000).
31. Sia, C. M., Pearson, J. S., Howden, B. P., Williamson, D. A. & Ingle, D. J. Salmonella pathogenicity islands in the genomic era. *Trends in Microbiology* **33**, 752–764 (2025).
32. Doublet, B., Boyd, D., Mulvey, M. R. & Cloeckaert, A. The *Salmonella* genomic island 1 is an integrative mobilizable element. *Molecular Microbiology* **55**, 1911–1924 (2005).
33. Durrant, M. G., Li, M. M., Siranosian, B. A., Montgomery, S. B. & Bhatt, A. S. A Bioinformatic Analysis of Integrative Mobile Genetic Elements Highlights Their Role in Bacterial Adaptation. *Cell Host & Microbe* **27**, 140-153.e9 (2020).
34. Hussain, F. A. *et al.* Rapid evolutionary turnover of mobile genetic elements drives bacterial resistance to phages. *Science* **374**, 488–492 (2021).
35. Ares-Arroyo, M., Nucci, A. & Rocha, E. P. C. Expanding the diversity of origin of transfer-containing sequences in mobilizable plasmids. *Nat Microbiol* **9**, 3240–3253 (2024).
36. Guglielmini, J. *et al.* Key components of the eight classes of type IV secretion systems involved in bacterial conjugation or protein secretion. *Nucleic Acids Research* **42**, 5715–5727 (2014).
37. Kiss, J. *et al.* Identification and Characterization of oriT and Two Mobilization Genes Required for Conjugative Transfer of Salmonella Genomic Island 1. *Front. Microbiol.* **10**, 457 (2019).
38. Lorenzo-Díaz, F., Fernández-López, C., Guillén-Guío, B., Bravo, A. & Espinosa, M. Relaxase MobM Induces a Molecular Switch at Its Cognate Origin of Transfer. *Front. Mol. Biosci.* **5**, 17 (2018).
39. Nowak, K. P. *et al.* Molecular and Functional Characterization of MobK Protein—A Novel-Type Relaxase Involved in Mobilization for Conjugational Transfer of Klebsiella pneumoniae Plasmid pIGRK. *IJMS* **22**, 5152 (2021).
40. Wisniewski, J. A. *et al.* TcpM: a novel relaxase that mediates transfer of large conjugative plasmids from *Clostridium perfringens*. *Molecular Microbiology* **99**, 884–896 (2016).
41. Oliveira, P. H., Touchon, M., Cury, J. & Rocha, E. P. C. The chromosomal organization of horizontal gene transfer in bacteria. *Nat Commun* **8**, 841 (2017).
42. Garcillán-Barcia, M. P., de la Cruz, F. & Rocha, E. P. C. The extended mobility of plasmids. *Nucleic Acids Research* **53**, gkaf652 (2025).
43. Fekete, R. A. & Frost, L. S. Mobilization of Chimeric *oriT* Plasmids by F and R100-1: Role of Relaxosome Formation in Defining Plasmid Specificity. *J Bacteriol* **182**, 4022–4027 (2000).
44. Avila, P., Núñez, B. & de la Cruz, F. Plasmid R6K contains two functional oriTs which can assemble simultaneously in relaxosomes in vivo. *J Mol Biol* **261**, 135–143 (1996).
45. Miyazaki, R. & Van Der Meer, J. R. A dual functional origin of transfer in the ICEclc genomic island of Pseudomonas knackmussii B13: oriT of ICEclc. *Molecular Microbiology* **79**, 743–758 (2011).
46. Cury, J., Oliveira, P. H., de la Cruz, F. & Rocha, E. P. C. Host Range and Genetic Plasticity Explain the Coexistence of Integrative and Extrachromosomal Mobile Genetic Elements. *Molecular Biology and Evolution* **35**, 2230–2239 (2018).
47. Yu, S. L. *et al.* The TIGER/Islander resource for genomic islands. *Microbiol Resour Announc* **14**, e00492-25 (2025).
48. Cury, J., Touchon, M. & Rocha, E. P. C. Integrative and conjugative elements and their hosts: composition, distribution and organization. *Nucleic Acids Res* **45**, 8943–8956 (2017).

49. Coluzzi, C., Garcillán-Barcia, M. P., de la Cruz, F. & Rocha, E. P. C. Evolution of Plasmid Mobility: Origin and Fate of Conjugative and Nonconjugative Plasmids. *Molecular Biology and Evolution* **39**, msac115 (2022).
50. Daccord, A., Ceccarelli, D. & Burrus, V. Integrating conjugative elements of the SXT/R391 family trigger the excision and drive the mobilization of a new class of Vibrio genomic islands: ICE-mediated GI mobilization. *Molecular Microbiology* **78**, 576–588 (2010).
51. Douard, G., Praud, K., Cloeckaert, A. & Doublet, B. The Salmonella Genomic Island 1 Is Specifically Mobilized In Trans by the IncA/C Multidrug Resistance Plasmid Family. *PLoS ONE* **5**, e15302 (2010).
52. Geng, P. *et al.* Horizontal transfer of large plasmid with type IV secretion system and mosquitocidal genomic island with excision and integration capabilities in *Lysinibacillus sphaericus*. *Environmental Microbiology* **23**, 5131–5146 (2021).
53. Valentine, P. J., Shoemaker, N. B. & Salyers, A. A. Mobilization of Bacteroides plasmids by Bacteroides conjugal elements. *J Bacteriol* **170**, 1319–1324 (1988).
54. Wong, J. *et al.* The assembly of a hybrid type IV secretion system by a Crohn's disease-associated Escherichia coli strain. *Nat Commun* **16**, 8797 (2025).
55. Taylor, D. E. *et al.* Genomic Variability of O Islands Encoding Tellurite Resistance in Enterohemorrhagic *Escherichia coli* O157:H7 Isolates. *J Bacteriol* **184**, 4690–4698 (2002).
56. Neupane, D. P., Bearson, B. L. & Bearson, S. M. D. Localization of the origin of transfer (*oriT*) for *Salmonella* Genomic Island 4 (SGI-4) from *Salmonella enterica* serovar I 4, [5],12:i:-. *DNA Research* dsaf023 (2025) doi:10.1093/dnares/dsaf023.
57. Miruna Perta, A. *et al.* Integrative mobilizable elements are pervasive throughout Pseudomonadota. Preprint at https://doi.org/10.64898/2026.01.12.698999 (2026).
58. Lin, T.-L., Lee, C.-Z., Hsieh, P.-F., Tsai, S.-F. & Wang, J.-T. Characterization of Integrative and Conjugative Element ICE *Kp1* -Associated Genomic Heterogeneity in a *Klebsiella pneumoniae* Strain Isolated from a Primary Liver Abscess. *J Bacteriol* **190**, 515–526 (2008).
59. Beamud, B., Benz, F. & Bikard, D. Going viral: The role of mobile genetic elements in bacterial immunity. *Cell Host & Microbe* **32**, 804–819 (2024).
60. Shaw, L. P., Rocha, E. P. C. & MacLean, R. C. Restriction-modification systems have shaped the evolution and distribution of plasmids across bacteria. *Nucleic Acids Research* **51**, 6806–6818 (2023).
61. Jaskólska, M., Adams, D. W. & Blokesch, M. Two defence systems eliminate plasmids from seventh pandemic Vibrio cholerae. *Nature* **604**, 323–329 (2022).
62. Couturier, A. *et al.* Real-time visualisation of the intracellular dynamics of conjugative plasmid transfer. *Nat Commun* **14**, 294 (2023).
63. Samuel, B., Mittelman, K., Croitoru, S. Y., Ben Haim, M. & Burstein, D. Diverse anti-defence systems are encoded in the leading region of plasmids. *Nature* **635**, 186–192 (2024).
64. Marcoleta, A. E., Berríos-Pastén, C., Nuñez, G., Monasterio, O. & Lagos, R. Klebsiella pneumoniae Asparagine tDNAs Are Integration Hotspots for Different Genomic Islands Encoding Microcin E492 Production Determinants and Other Putative Virulence Factors Present in Hypervirulent Strains. *Front. Microbiol.* **7**, (2016).
65. Rivard, N., Colwell, R. R. & Burrus, V. Antibiotic Resistance in Vibrio cholerae: Mechanistic Insights from IncC Plasmid-Mediated Dissemination of a Novel Family of Genomic Islands Inserted at *trmE*. *mSphere* **5**, 10.1128/msphere.00748-20 (2020).
66. Bellanger, X. *et al.* Site-specific accretion of an integrative conjugative element together with a related genomic island leads to *cis* mobilization and gene capture. *Molecular Microbiology* **81**, 912–925 (2011).
67. Ray, M. D., Boundy, S. & Archer, G. L. Transfer of the methicillin resistance genomic island among staphylococci by conjugation. *Molecular Microbiology* **100**, 675–685 (2016).
68. Libante, V. *et al.* Mobilization of IMEs Integrated in the oriT of ICEs Involves Their Own Relaxase Belonging to the Rep-Trans Family of Proteins. *Genes* **11**, 1004 (2020).
69. Hua, M. *et al.* A chromosome-encoded T4SS independently contributes to horizontal gene transfer in Enterococcus faecalis. *Cell Reports* **41**, 111609 (2022).
70. Whittle, G., Hamburger, N., Shoemaker, N. B. & Salyers, A. A. A *Bacteroides* Conjugative Transposon, CTnERL, Can Transfer a Portion of Itself by Conjugation without Excising from the Chromosome. *J Bacteriol* **188**, 1169–1174 (2006).
71. Deep, A. *et al.* The SMC-family Wadjet complex protects bacteria from plasmid transformation by recognition and cleavage of closed-circular DNA. *Molecular Cell* **82**, 4145-4159.e7 (2022).
72. Zongo, P. D. *et al.* An antiplasmid system drives antibiotic resistance gene integration in carbapenemase-producing Escherichia coli lineages. *Nat Commun* **15**, 4093 (2024).

73. Redondo-Salvo, S. *et al.* Pathways for horizontal gene transfer in bacteria revealed by a global map of their plasmids. *Nat Commun* **11**, 3602 (2020).
74. Carraro, N., Poulin, D. & Burrus, V. Replication and Active Partition of Integrative and Conjugative Elements (ICEs) of the SXT/R391 Family: The Line between ICEs and Conjugative Plasmids Is Getting Thinner. *PLoS Genet* **11**, e1005298 (2015).
75. Delavat, F., Miyazaki, R., Carraro, N., Pradervand, N. & Van Der Meer, J. R. The hidden life of integrative and conjugative elements. *FEMS Microbiology Reviews* **41**, 512–537 (2017).
76. Meyer, R. The r1162 mob proteins can promote conjugative transfer from cryptic origins in the bacterial chromosome. *J Bacteriol* **191**, 1574–1580 (2009).
77. Ramsay, J. P. *et al.* A widely conserved molecular switch controls quorum sensing and symbiosis island transfer in *M esorhizobium loti* through expression of a novel antiactivator. *Molecular Microbiology* **87**, 1–13 (2013).
78. Burrus, V. & Waldor, M. K. Control of SXT Integration and Excision. *J Bacteriol* **185**, 5045–5054 (2003).
79. Waters, J. L. & Salyers, A. A. Regulation of CTnDOT Conjugative Transfer Is a Complex and Highly Coordinated Series of Events. *mBio* **4**, e00569-13 (2013).
80. Verdonk, C. J. *et al.* Structural basis for control of integrative and conjugative element excision and transfer by the oligomeric winged helix–turn–helix protein RdfS. *Nucleic Acids Research* **53**, gkaf249 (2025).
81. Pfeifer, E. & Rocha, E. P. C. Phage-plasmids promote recombination and emergence of phages and plasmids. *Nat Commun* **15**, 1545 (2024).
82. Wozniak, R. A. F. & Waldor, M. K. Integrative and conjugative elements: mosaic mobile genetic elements enabling dynamic lateral gene flow. *Nat Rev Microbiol* **8**, 552–563 (2010).
83. Jacob, F. & Wollman, E. L. Genetic and physical determinations of chromosomal segments in Escherichia coli. *Symp Soc Exp Biol* **12**, 75–92 (1958).
84. Errington, J. & Pughe, N. Upper limit for DNA packaging by Bacillus subtilis bacteriophage φ 105: Isolation of phage deletion mutants by induction of oversized prophages. *Molec Gen Genet* **210**, 347–351 (1987).
85. Humphrey, S. *et al.* Staphylococcal phages and pathogenicity islands drive plasmid evolution. *Nat Commun* **12**, 5845 (2021).
86. Coluzzi, C. & Rocha, E. P. C. The Spread of Antibiotic Resistance Is Driven by Plasmids Among the Fastest Evolving and of Broadest Host Range. *Molecular Biology and Evolution* **42**, msaf060 (2025).
87. Zheng, Q., Li, L., Yin, X., Che, Y. & Zhang, T. Is ICE hot? A genomic comparative study reveals integrative and conjugative elements as "hot" vectors for the dissemination of antibiotic resistance genes. *mSystems* **8**, e00178-23 (2023).
88. Enault, F. *et al.* Phages rarely encode antibiotic resistance genes: a cautionary tale for virome analyses. *The ISME Journal* **11**, 237–247 (2017).
89. Pfeifer, E., Bonnin, R. & Rocha, E. P. C. *Phage-Plasmids Spread Antibiotic Resistance Genes through Infection and Lysogenic Conversion*. http://biorxiv.org/lookup/doi/10.1101/2022.06.24.497495 (2022) doi:10.1101/2022.06.24.497495.
90. Hyatt, D. *et al.* Prodigal: prokaryotic gene recognition and translation initiation site identification. *BMC Bioinformatics* **11**, 119 (2010).
91. Cantalapiedra, C. P., Hernández-Plaza, A., Letunic, I., Bork, P. & Huerta-Cepas, J. eggNOG-mapper v2: Functional Annotation, Orthology Assignments, and Domain Prediction at the Metagenomic Scale. *Molecular Biology and Evolution* **38**, 5825–5829 (2021).
92. Néron, B. *et al.* MacSyFinder v2: Improved modelling and search engine to identify molecular systems in genomes. *Peer Community Journal* **3**, e28 (2023).
93. Tesson, F. *et al.* Systematic and quantitative view of the antiviral arsenal of prokaryotes. *Nat Commun* **13**, 2561 (2022).
94. Tesson, F. *et al.* A Comprehensive Resource for Exploring Antiphage Defense: DefenseFinder Webservice,Wiki and Databases. *Peer Community Journal* **4**, e91 (2024).
95. Feldgarden, M. *et al.* AMRFinderPlus and the Reference Gene Catalog facilitate examination of the genomic links among antimicrobial resistance, stress response, and virulence. *Sci Rep* **11**, 12728 (2021).
96. Camacho, C. *et al.* BLAST+: architecture and applications. *BMC Bioinformatics* **10**, 421 (2009).
97. Zhou, S., Liu, B., Zheng, D., Chen, L. & Yang, J. VFDB 2025: an integrated resource for exploring anti-virulence compounds. *Nucleic Acids Research* **53**, D871–D877 (2025).
98. Xie, Z. & Tang, H. ISEScan: automated identification of insertion sequence elements in prokaryotic genomes. *Bioinformatics* **33**, 3340–3347 (2017).
99. Mistry, J. *et al.* Pfam: The protein families database in 2021. *Nucleic Acids Res* **49**, D412–D419 (2021).

100. Liu, G. *et al.* oriTDB: a database of the origin-of-transfer regions of bacterial mobile genetic elements. *Nucleic Acids Research* **53**, D163–D168 (2025).
101. Núñez, B. & De La Cruz, F. Two atypical mobilization proteins are involved in plasmid CloDF13 relaxation. *Molecular Microbiology* **39**, 1088–1099 (2001).
102. Francia, M. V. & Clewell, D. B. Transfer origins in the conjugative *Enterococcus faecalis* plasmids pAD1 and pAM373: identification of the pAD1 *nic* site, a specific relaxase and a possible TraG-like protein. *Molecular Microbiology* **45**, 375–395 (2002).
103. Pearson, W. R. & Lipman, D. J. Improved tools for biological sequence comparison. *Proc. Natl. Acad. Sci. U.S.A.* **85**, 2444–2448 (1988).
104. Steinegger, M. & Söding, J. MMseqs2 enables sensitive protein sequence searching for the analysis of massive data sets. *Nat Biotechnol* **35**, 1026–1028 (2017).
105. Katoh, K. & Standley, D. M. MAFFT Multiple Sequence Alignment Software Version 7: Improvements in Performance and Usability. *Molecular Biology and Evolution* **30**, 772–780 (2013).
106. Carraro, N. *et al.* Development of pVCR94ΔX from Vibrio cholerae, a prototype for studying multidrug resistant IncA/C conjugative plasmids. *Front. Microbiol.* **5**, 5:44 (2014).
107. Ceccarelli, D., Daccord, A., René, M. & Burrus, V. Identification of the Origin of Transfer (*oriT*) and a New Gene Required for Mobilization of the SXT/R391 Family of Integrating Conjugative Elements. *J Bacteriol* **190**, 5328–5338 (2008).
108. Tian, D. *et al.* Prevalence of hypervirulent and carbapenem-resistant *Klebsiella pneumoniae* under divergent evolutionary patterns. *Emerging Microbes & Infections* **11**, 1936–1949 (2022).
109. Shen, W., Le, S., Li, Y. & Hu, F. SeqKit: A Cross-Platform and Ultrafast Toolkit for FASTA/Q File Manipulation. *PLoS ONE* **11**, e0163962 (2016).
110. Wheeler, T. J. & Eddy, S. R. nhmmer: DNA homology search with profile HMMs. *Bioinformatics* **29**, 2487–2489 (2013).
111. Fricke, W. F. *et al.* Comparative Genomics of the IncA/C Multidrug Resistance Plasmid Family. *J Bacteriol* **191**, 4750–4757 (2009).
112. Hegyi, A., Szabó, M., Olasz, F. & Kiss, J. Identification of oriT and a recombination hot spot in the IncA/C plasmid backbone. *Sci Rep* **7**, 10595 (2017).
113. Ilchenko, K., Bonnin, R. A., Rocha, E. P. & Pfeifer, E. Efficient detection and typing of phage-plasmids. Preprint at https://doi.org/10.1101/2025.08.29.673033 (2025).
114. Redondo-Salvo, S. *et al.* COPLA, a taxonomic classifier of plasmids. *BMC Bioinformatics* **22**, 390 (2021).
115. Garcillán-Barcia, M. P., Redondo-Salvo, S. & De La Cruz, F. Plasmid classifications. *Plasmid* **126**, 102684 (2023).
116. Garcillán-Barcia, M. P., Francia, M. V. & de La Cruz, F. The diversity of conjugative relaxases and its application in plasmid classification. *FEMS Microbiol Rev* **33**, 657–687 (2009).
117. Perrin, A. & Rocha, E. P. C. PanACoTA: a modular tool for massive microbial comparative genomics. *NAR Genom Bioinform* **3**, lqaa106 (2021).
118. Rajeev, L., Malanowska, K. & Gardner, J. F. Challenging a Paradigm: the Role of DNA Homology in Tyrosine Recombinase Reactions. *Microbiol Mol Biol Rev* **73**, 300–309 (2009).
119. Pavlovic, G., Burrus, V., Gintz, B., Decaris, B. & Guédon, G. Evolution of genomic islands by deletion and tandem accretion by site-specific recombination: ICESt1-related elements from Streptococcus thermophilus. *Microbiology* **150**, 759–774 (2004).
120. Ambroset, C. *et al.* New Insights into the Classification and Integration Specificity of Streptococcus Integrative Conjugative Elements through Extensive Genome Exploration. *Front. Microbiol.* **6**, (2016).
121. Tommasini, D., Mageeney, C. M. & Williams, K. P. Helper-embedded satellites from an integrase clade that repeatedly targets prophage late genes. *NAR Genomics and Bioinformatics* **5**, lqad036 (2023).
122. Csárdi, G. *et al.* igraph for R: R interface of the igraph library for graph theory and network analysis. Zenodo https://doi.org/10.5281/ZENODO.7682609 (2025).
123. Bastian, M., Heymann, S. & Jacomy, M. Gephi: An Open Source Software for Exploring and Manipulating Networks. *ICWSM* **3**, 361–362 (2009).
124. Ares-Arroyo, M. HMM profiles for the screening of conjugative origins of transfer. 8143879 Bytes figshare https://doi.org/10.6084/M9.FIGSHARE.31047685 (2026).
125. Ares-Arroyo, M. R Scripts for the identification of sequences containing origins of transfer by conjugation. 37685 Bytes figshare https://doi.org/10.6084/M9.FIGSHARE.26870155.V1 (2024).

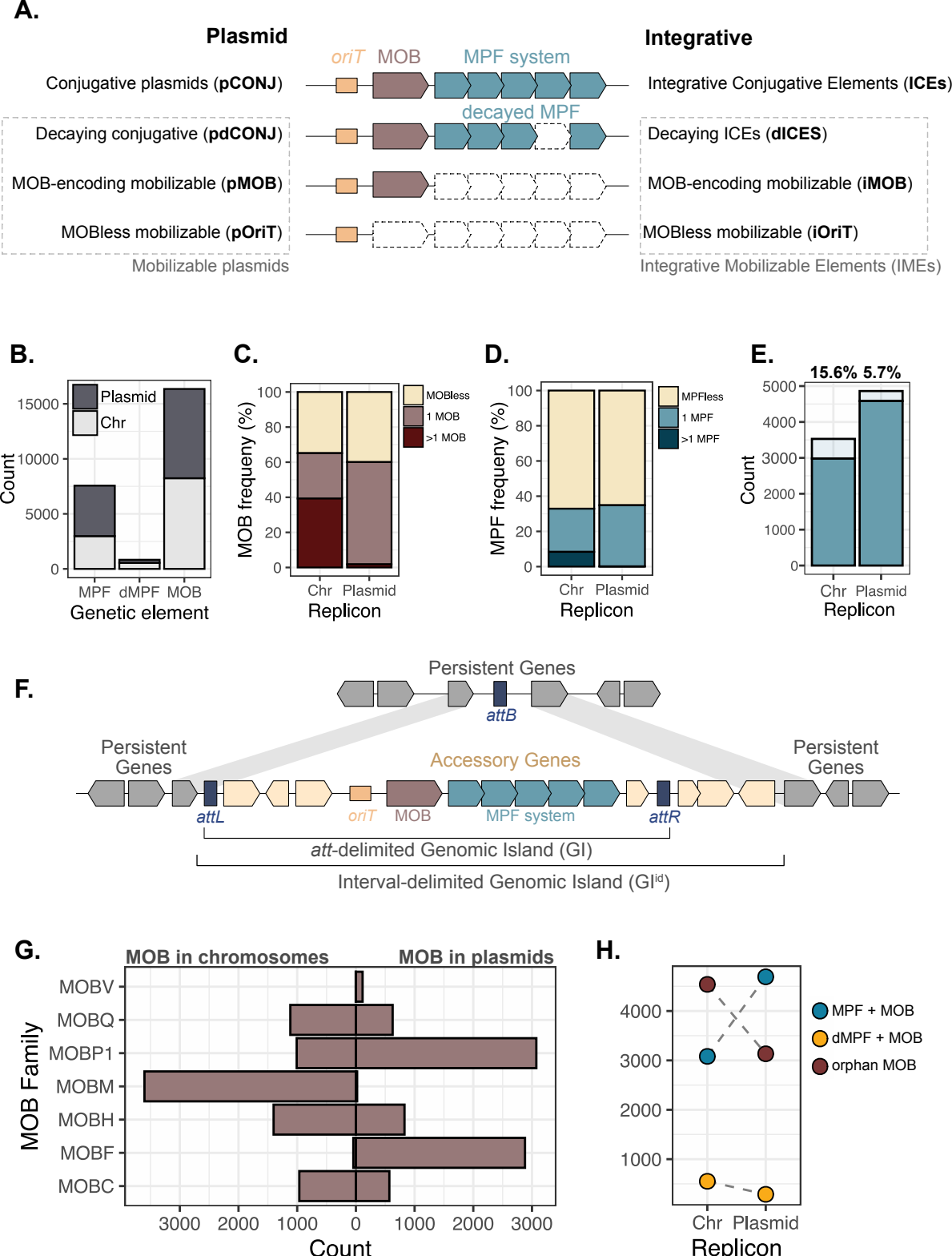
A.
Plasmid
Integrative
oriT
MOB
MPF system
decayed MPF
Conjugative plasmids (pCONJ)
Decaying conjugative (pdCONJ)
MOB-encoding mobilizable (pMOB)
MOBless mobilizable (pOriT)
Mobilizable plasmids
Integrative Conjugative Elements (ICEs)
Decaying ICEs (dICES)
MOB-encoding mobilizable (iMOB)
MOBless mobilizable (iOriT)
Integrative Mobilizable Elements (IMEs)
B.
Plasmid
Chr
Count
MPF
dMPF
MOB
Genetic element
C.
MOB frequency (%)
MOBless
1 MOB
>1 MOB
Chr
Plasmid
Replicon
D.
MPF frequency (%)
MPFless
1 MPF
>1 MPF
Chr
Plasmid
Replicon
E.
15.6% 5.7%
Count
Chr
Plasmid
Replicon
F.
Persistent Genes
attB
Persistent Genes
Accessory Genes
Persistent Genes
attL
oriT
MOB
MPF system
attR
att-delimited Genomic Island (GI)
Interval-delimited Genomic Island (GIid)
G.
MOB in chromosomes
MOB in plasmids
MOB Family
MOBV
MOBQ
MOBP1
MOBM
MOBH
MOBF
MOBC
Count
H.
MPF + MOB
dMPF + MOB
orphan MOB
Chr
Plasmid
Replicon

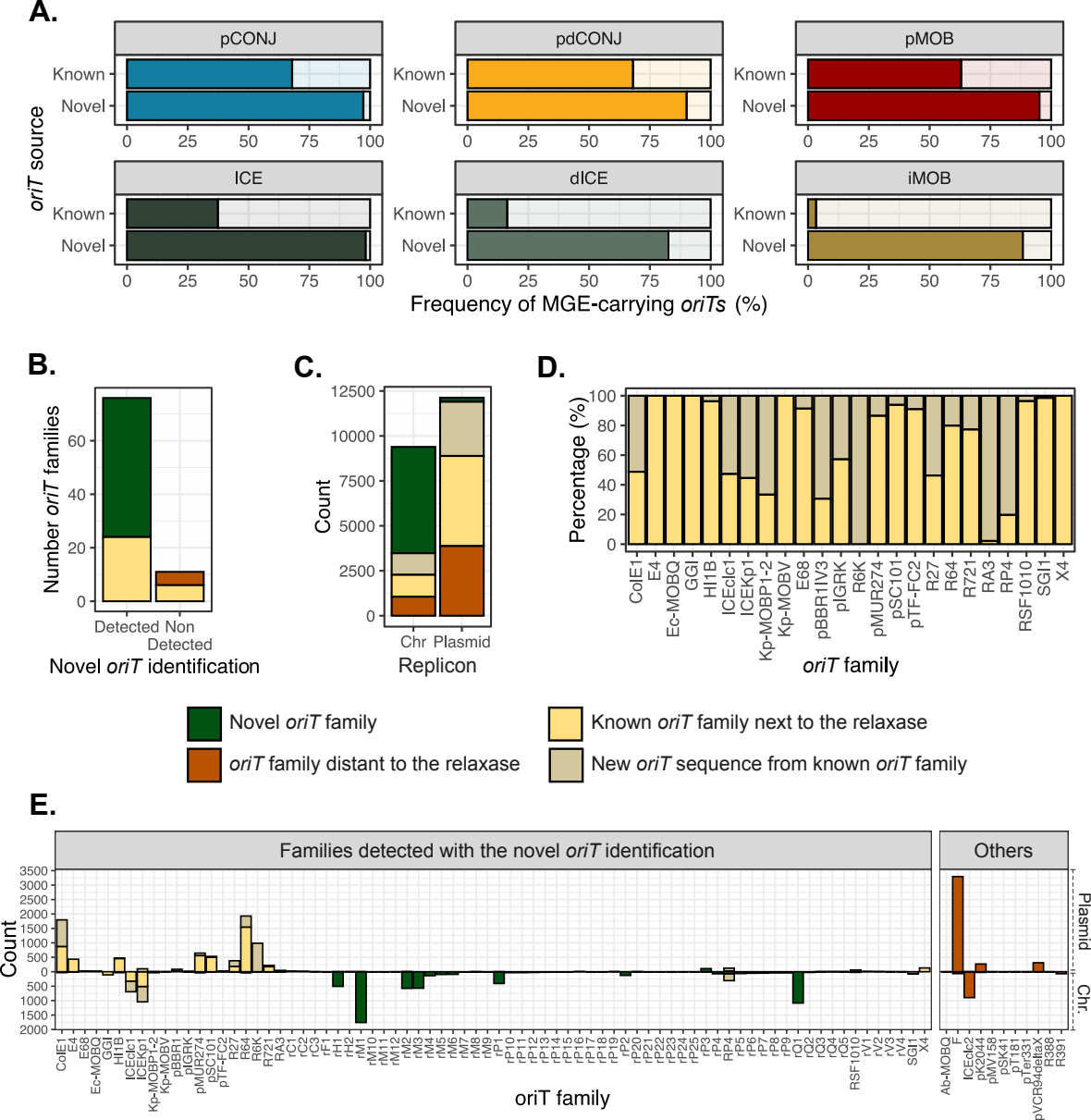
A.
pCONJ
pdCONJ
pMOB
ICE
dICE
iMOB
Known
Novel
oriT source
0
25
50
75
100
Frequency of MGE-carrying oriTs (%)
B.
Number oriT families
Detected
Non Detected
Novel oriT identification
C.
Count
Chr
Plasmid
Replicon
D.
Percentage (%)
ColE1
E4
Ec-MOBQ
GGI
HI1B
ICEdc1
ICEKp1
Kp-MOBP1-2
Kp-MOBV
E68
pBBR1IV3
pIGRK
R6K
pMUR274
pSC101
pTF-FC2
R27
R64
R721
RA3
RP4
RSF1010
SGI1
X4
oriT family
Novel oriT family
oriT family distant to the relaxase
Known oriT family next to the relaxase
New oriT sequence from known oriT family
E.
Families detected with the novel oriT identification
Others
Count
Plasmid
Chr.
oriT family

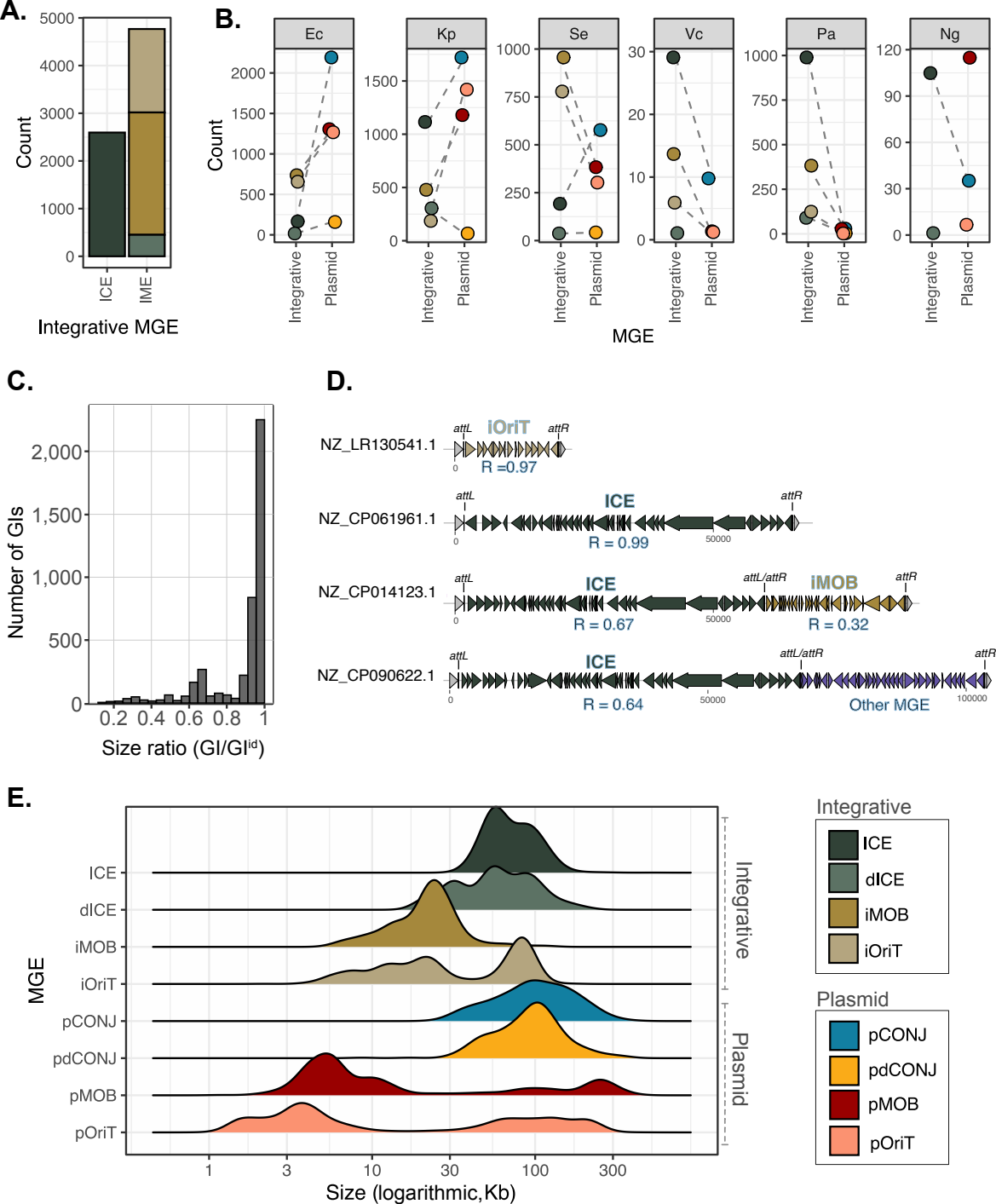
A.
Count
ICE
IME
Integrative MGE
B.
Ec
Kp
Se
Vc
Pa
Ng
Count
Integrative
Plasmid
MGE
C.
Number of GIs
Size ratio (GI/GI^id)
D.
NZ_LR130541.1
NZ_CP061961.1
NZ_CP014123.1
NZ_CP090622.1
attL
attR
iOriT
ICE
iMOB
attL/attR
R =0.97
R = 0.99
R = 0.67
R = 0.32
R = 0.64
Other MGE
E.
MGE
ICE
dICE
iMOB
iOriT
pCONJ
pdCONJ
pMOB
pOriT
Integrative
Plasmid
Size (logarithmic,Kb)
Integrative
ICE
dICE
iMOB
iOriT
Plasmid
pCONJ
pdCONJ
pMOB
pOriT

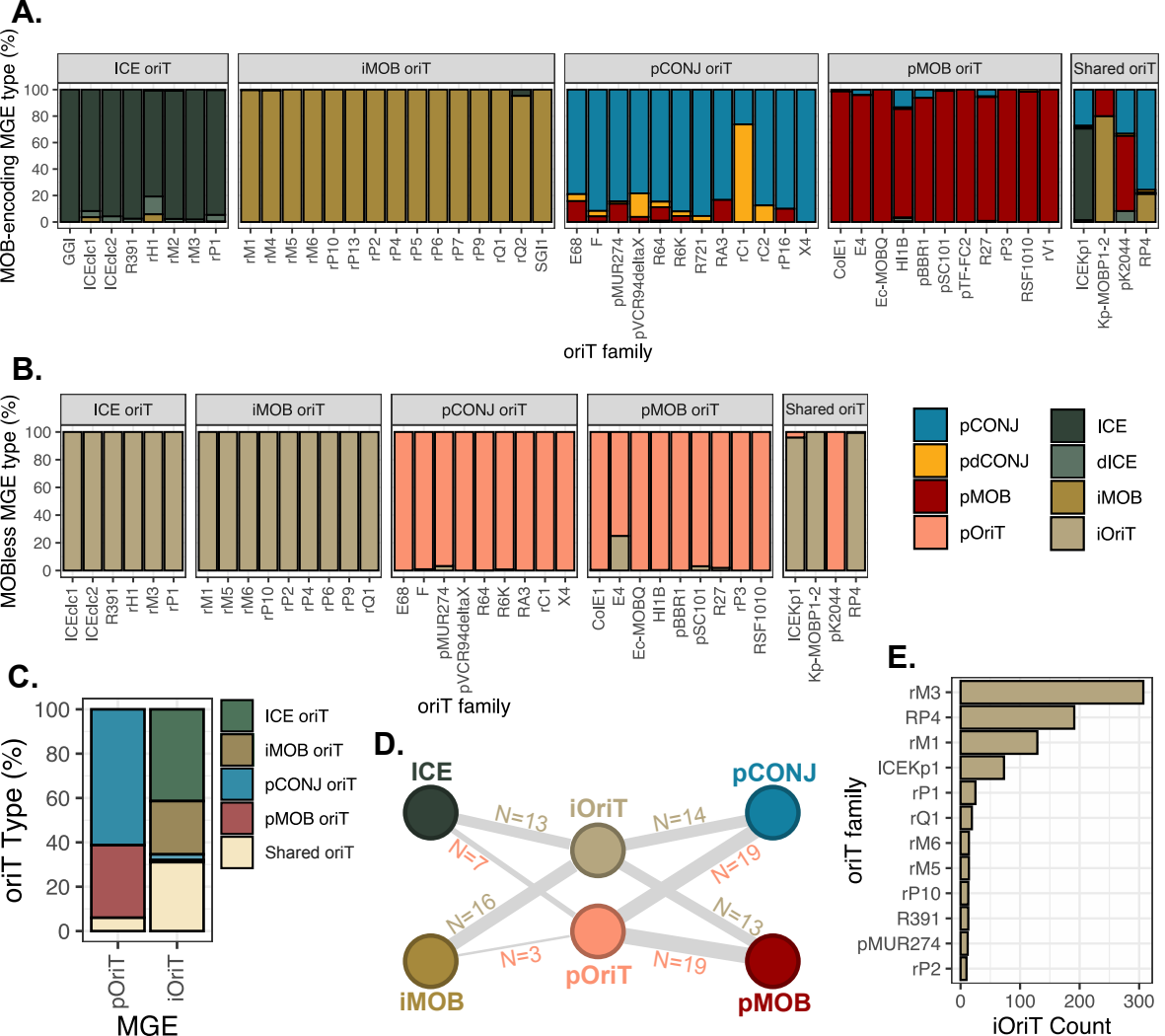
A.
MOB-encoding MGE type (%)
ICE oriT
iMOB oriT
pCONJ oriT
pMOB oriT
Shared oriT
GGI
ICEdc1
ICEdc2
R391
rH1
rM2
rM3
rP1
rM1
rM4
rM5
rM6
rP10
rP13
rP2
rP4
rP5
rP6
rP7
rP9
rQ1
rQ2
SGI1
E68
F
pMUR274
pVCR94deltaX
R64
R6K
R721
RA3
rC1
rC2
rP16
X4
ColE1
E4
Ec-MOBQ
HI1B
pBBR1
pSC101
pTF-FC2
R27
rP3
RSF1010
rV1
ICEKp1
Kp-MOBP1-2
pK2044
RP4
oriT family
B.
MOBless MGE type (%)
pCONJ
pdCONJ
pMOB
pOriT
ICE
dICE
iMOB
iOriT
C.
oriT Type (%)
ICE oriT
iMOB oriT
pCONJ oriT
pMOB oriT
Shared oriT
pOriT
iOriT
MGE
D.
ICE
iOriT
pCONJ
iMOB
pOriT
pMOB
N=13
N=14
N=7
N=19
N=16
N=13
N=3
N=19
E.
oriT family
rM3
RP4
rM1
ICEKp1
rP1
rQ1
rM6
rM5
rP10
R391
pMUR274
rP2
iOriT Count

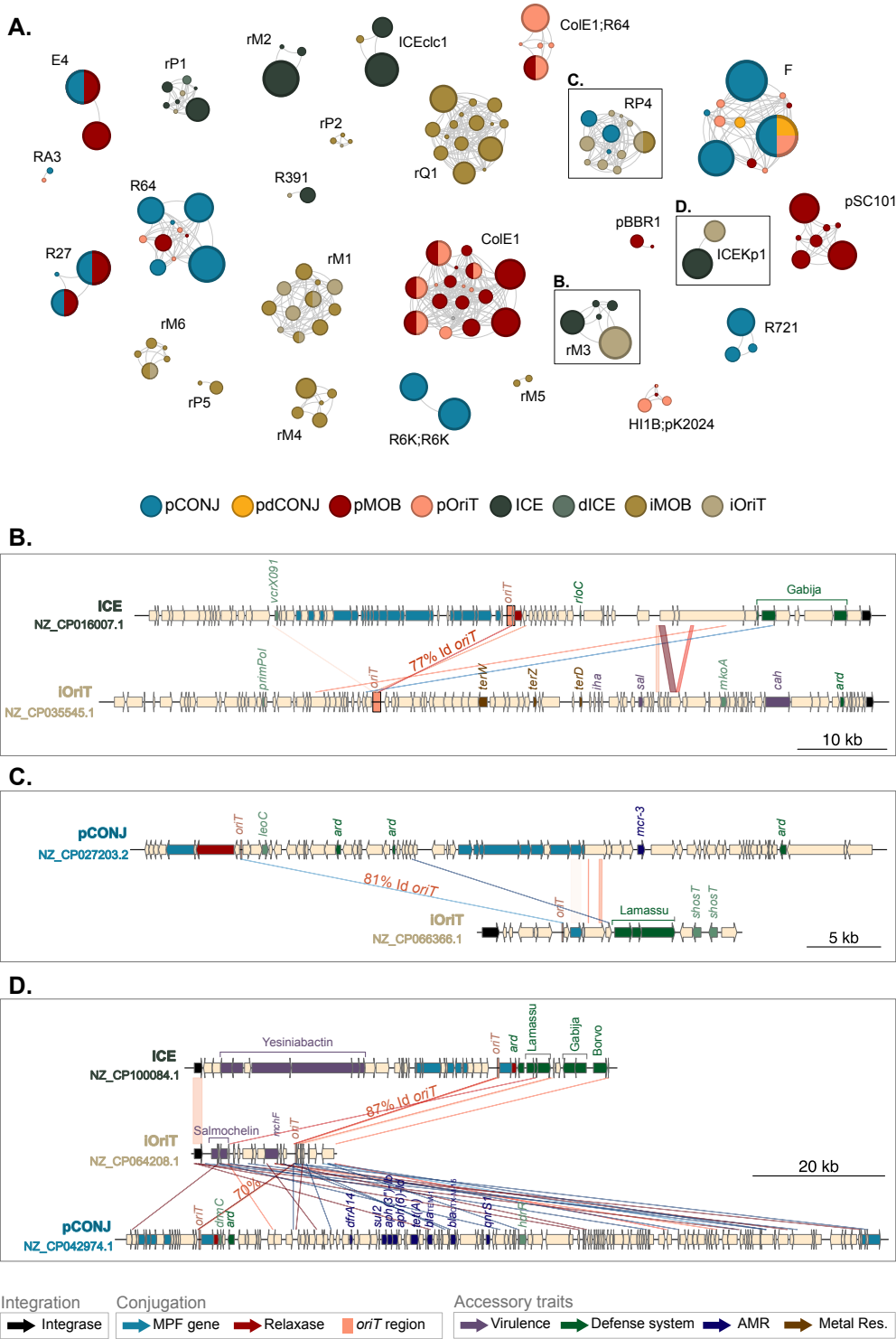
A.
E4
rP1
rM2
ICEclc1
ColE1;R64
C.
RP4
F
RA3
rP2
rQ1
R64
R391
D.
pSC101
pBBR1
ICEKp1
R27
rM1
ColE1
B.
rM3
R721
rM6
rP5
rM4
R6K;R6K
rM5
HI1B;pK2024
pCONJ
pdCONJ
pMOB
pOriT
ICE
dICE
iMOB
iOriT
B.
ICE
NZ_CP016007.1
vcrX091
oriT
rloC
Gabija
77% Id oriT
iOriT
NZ_CP035545.1
primPol
oriT
terW
terZ
terD
iha
sal
mkoA
cah
ard
10 kb
C.
pCONJ
NZ_CP027203.2
oriT
leoC
ard
ard
mcr-3
ard
81% Id oriT
iOriT
NZ_CP066366.1
oriT
Lamassu
shosT
shosT
5 kb
D.
ICE
NZ_CP100084.1
Yesiniabactin
oriT
ard
Lamassu
Gabija
Borvo
87% Id oriT
iOriT
NZ_CP064208.1
Salmochelin
mchF
oriT
20 kb
70%
pCONJ
NZ_CP042974.1
oriT
drmC
ard
dfrA14
sul2
aph(3'')-Ib
aph(6)-Id
tet(A)
blaTEM
blaCTX-M-15
qnrS1
hcrR
Integration
Integrase
Conjugation
MPF gene
Relaxase
oriT region
Accessory traits
Virulence
Defense system
AMR
Metal Res.

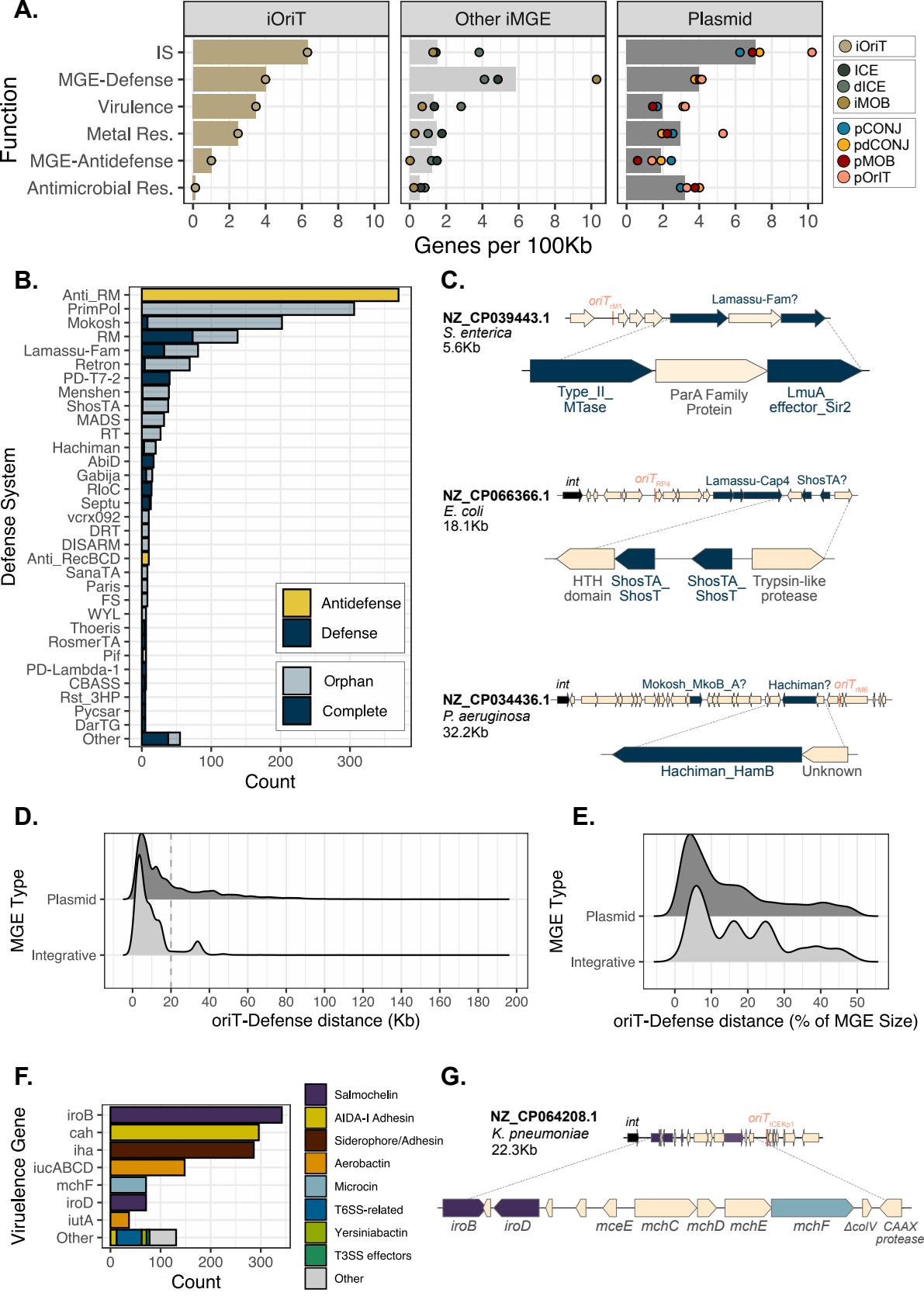
A.
iOriT
Other iMGE
Plasmid
Function
IS
MGE-Defense
Virulence
Metal Res.
MGE-Antidefense
Antimicrobial Res.
Genes per 100Kb
iOriT
ICE
dICE
iMOB
pCONJ
pdCONJ
pMOB
pOrIT
B.
Defense System
Anti_RM
PrimPol
Mokosh
RM
Lamassu-Fam
Retron
PD-T7-2
Menshen
ShosTA
MADS
RT
Hachiman
AbiD
Gabija
RloC
Septu
vcrx092
DRT
DISARM
Anti_RecBCD
SanaTA
Paris
FS
WYL
Thoeris
RosmerTA
Pif
PD-Lambda-1
CBASS
Rst_3HP
Pycsar
DarTG
Other
Antidefense
Defense
Orphan
Complete
Count
C.
NZ_CP039443.1
S. enterica
5.6Kb
Lamassu-Fam?
Type_II_ MTase
ParA Family Protein
LmuA_ effector_Sir2
NZ_CP066366.1
E. coli
18.1Kb
int
Lamassu-Cap4
ShosTA?
HTH domain
ShosTA_ ShosT
ShosTA_ ShosT
Trypsin-like protease
NZ_CP034436.1
P. aeruginosa
32.2Kb
int
Mokosh_MkoB_A?
Hachiman?
Hachiman_HamB
Unknown
D.
MGE Type
Plasmid
Integrative
oriT-Defense distance (Kb)
E.
MGE Type
Plasmid
Integrative
oriT-Defense distance (% of MGE Size)
F.
Virulence Gene
iroB
cah
iha
iucABCD
mchF
iroD
iutA
Other
Count
Salmochelin
AIDA-I Adhesin
Siderophore/Adhesin
Aerobactin
Microcin
T6SS-related
Yersiniabactin
T3SS effectors
Other
G.
NZ_CP064208.1
K. pneumoniae
22.3Kb
int
iroB
iroD
mceE
mchC
mchD
mchE
mchF
ΔcolV
CAAX protease